

Linear Oligo(phenylenevinylene)-Based Covalent Organic Frameworks

Xingjiang Yu ^a, Yuelin Zhong ^a, Wenbo Dong ^a, Longyu Li^{*, a, b}

a. College of Polymer Science and Engineering, Sichuan University, Chengdu 610065, P. R. China

b. State Key Laboratory of Polymer Materials Engineering, Sichuan University, Chengdu 610065, P. R. China

Table of Contents

Section S1. General materials and methods	2
Section S2. Synthetic procedures	4
Section S3. Characterization data.....	18
Section S4. Electrochemical measurements	30
Section S5. Photocatalytic measurements	30
Section S6. Density functional theory (DFT) calculations	31
Section S7. Structural simulation	32
Reference.....	40

Section S1. General materials and methods

Materials

If not stated otherwise, all reagents were purchased from commercial sources and used without any further purification. Hydroquinone ($\geq 99\%$), iodomethane ($\geq 99\%$), α , α' -Dibromo-p-xylene ($\geq 99\%$), triethyl phosphite ($\geq 98\%$), 4-nitrobenzaldehyde ($\geq 98\%$), potassium tert-butoxide ($\geq 99\%$), sodium sulfide nonahydrate ($\geq 99\%$), acetic acid ($\geq 99\%$), ascorbic acid ($\geq 99\%$) were all purchased from Adamas (Shanghai). Tetrahydrofuran ($\geq 99.5\%$), methanol ($\geq 99.5\%$), ethanol ($\geq 99.5\%$), dichloromethane ($\geq 99.5\%$), mesitylene ($\geq 99\%$), 1,4-dioxane ($\geq 99.5\%$), n-butanol ($\geq 99.5\%$), o-dichlorobenzene ($\geq 98\%$), pyridine ($\geq 99.5\%$) dimethyl sulfoxide ($\geq 99.5\%$) were all purchased from Greagent (Shanghai). Acetone ($\geq 99.5\%$) and hydrochloric acid (37%) were purchased from CHRON CHEMICALS (Chengdu). Ltd. Nafion D-520 dispersion was purchased from Alfa Aesar.

Characterization

^1H NMR spectra were measured on a Bruker AVANCE III HD spectrometer operating at resonance frequencies of 400 MHz and are reported in ppm using solvent as an internal standard (CDCl_3 at 7.26 ppm for ^1H). Fourier transform infrared (FT-IR) spectra were recorded on a Nicolet NEXUS 670 spectrometer. The IR of the samples were collected with a universal diamond ATR (attenuated total reflection) in the $650 \sim 4000 \text{ cm}^{-1}$ region. Powder X-ray diffraction (PXRD) patterns were obtained on a MiniFlex 600 X-ray diffraction system (Cu , $K_{\alpha 1} = 1.540598$, $K_{\alpha 2} = 1.544426$, from 2° to 30° , step size = 0.01°) with focused radiation at 40 kV and 15 mA. Thermogravimetric analysis (TGA) from 30-800 $^\circ\text{C}$ was carried out on a METTLER TOLEDO TGA2 in a nitrogen atmosphere using a $10^\circ\text{C}/\text{min}$ ramp

without equilibration delay. The scanning electron microscope (SEM) was performed on a Thermo Scientific Helios 5 CX operating at an accelerating voltage ranging from 0.2 to 30 kV. Transmission Electron Microscope (TEM) was performed on a Thermo Scientific Talos F200X operating at a voltage 40 kV. COFs were activated using supercritical CO₂ with SCD-350M (Shianjia Technology). The surface areas and pore investigated by nitrogen adsorption and desorption at 77 K using iPore400 (PhysiChem Instruments Lid.). The pore-size distribution curves were obtained from the adsorption branches using non-local density functional theory (NLDFT) method. UV-visible absorption spectra of as-obtained materials were measured on a Shimadzu UV-2700 UV-vis spectrometer by measuring the reflectance of powders in the solid state. The scan was arranged from 200 to 800 nm with the scan rate of medium. Photoluminescence (PL) spectroscopy was recorded via the Fluorolog-3 spectrofluorometer (Horiba JobinYvon) at room temperature.

Section S2. Synthetic procedures

Synthesis of 1,4-bis(4-aminophenyl)vinyl)benzene (L-OPV-NH₂)

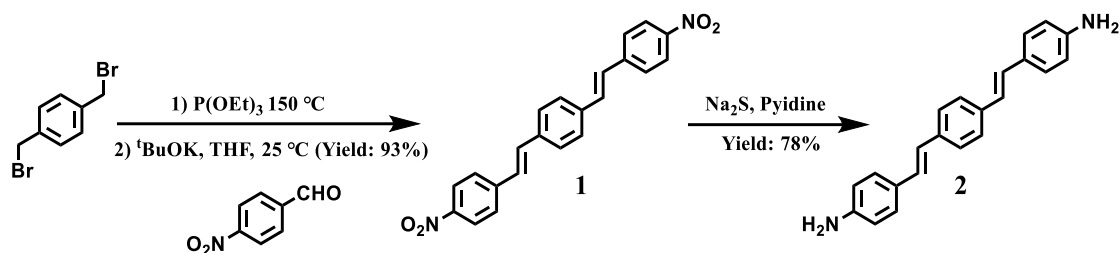


Figure S1. Synthetic routes of compound L-OPV-NH₂

Compound 1 and 2 was synthesized according to a literature method¹.

α, α' -Dibromo-p-xylene (1 g, 3.79 mmol) and triethyl phosphite (10 mL, 60.4 mmol) were added into a 100 mL single mouth bottle under nitrogen atmosphere, and heated at $150\text{ }^\circ\text{C}$ for 4 h. After cooling to room temperature, excess triethyl phosphite was removed under reduced pressure, and vacuumed until there are no liquid droplets left at the upper end of the condenser tube, to obtain a pale yellow oily compound. The obtained oily compound, THF (54 mL) and 4-nitrobenzaldehyde (2.29 g, 15.15 mmol) were added into a two necked flask in an ice water bath under nitrogen atmosphere, and the mixture was stirred for 20 min. After adding potassium tert-butoxide (2.55 g, 22.73 mmol) in batches, the mixture was transferred to room temperature for overnight reaction. Then 100 mL of water was added to quench, 5 mL of 3 M HCl was added to adjust pH to 2~3. After removing the solvent by evaporation, the resulting precipitate was filtered. The solid residue was washed by water, methanol, dichloromethane and acetone to afford a yellow powder (1.32 g, 93% yield). The obtained yellow solid is insoluble in chloroform and DMSO, and can be put into the next reaction without further purification.

Compound 1 (1.32 g, 3.55 mmol) was dissolved in 30 mL of pyridine and taken to ebullition. Then, a solution of $\text{Na}_2\text{S} \cdot 9\text{H}_2\text{O}$ (5.11 g, 21.28 mmol) in 14.2 mL of water was added while maintaining a gentle reflux. At this point, the color of the reaction mixture changes to dark brown. After the addition is complete, the reaction was stirred and heated at $115\text{ }^\circ\text{C}$ for 30 additional minutes. Then, the crude was poured over 100 mL of cold water. The solid product was filtered and washed by water to obtain a brown powder (0.86 g, 78% yield). ¹H NMR (400 MHz, DMSO-d₆, ppm): $\delta = 7.45$ (s, 4H), 7.26 (d, 4H), 7.02 (d, 2H), 6.89 (d, 2H), 6.57 (d, 4H), 5.30 (s, 4H).

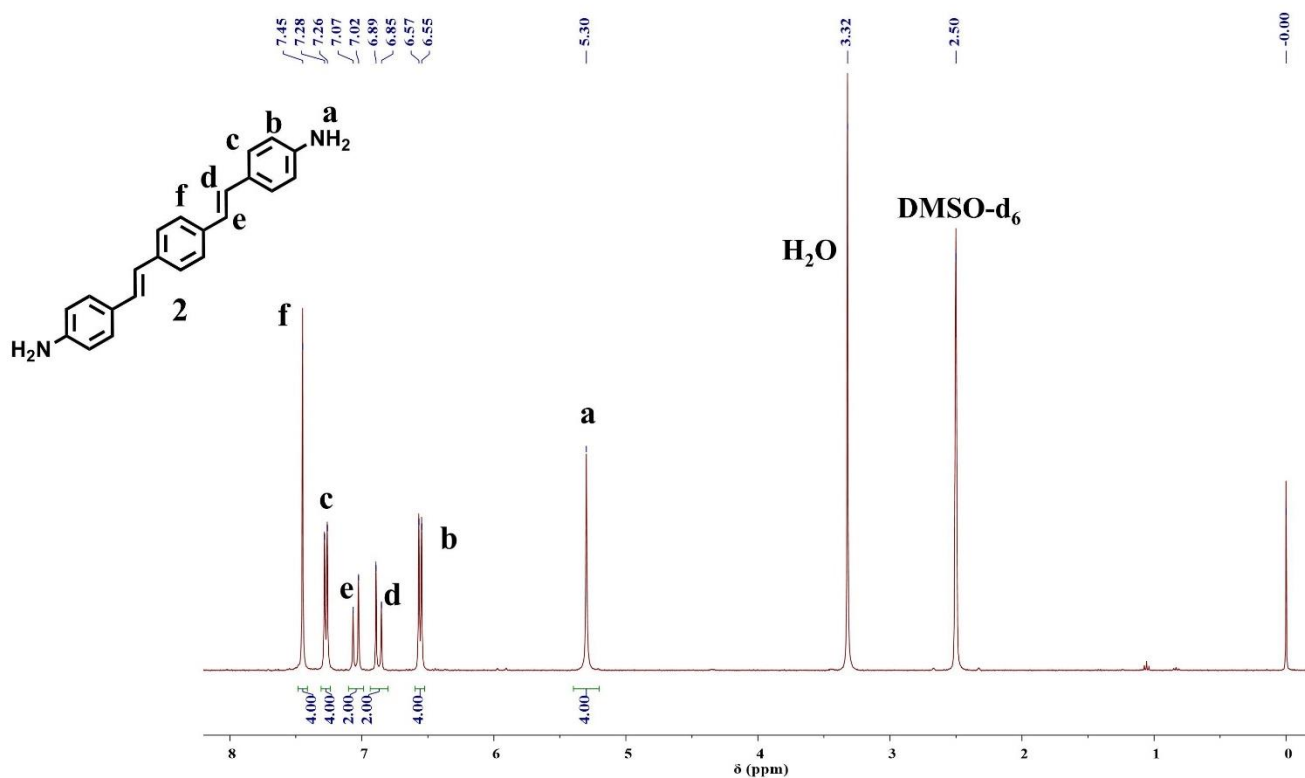


Figure S2. $^1\text{H-NMR}$ spectrum of L-OPV-NH₂ (2).

Synthesis of 2,5-Dimethoxy-1,4-bis(4-aminophenyl)vinyl)benzene (L-OPV-OMe-NH₂)

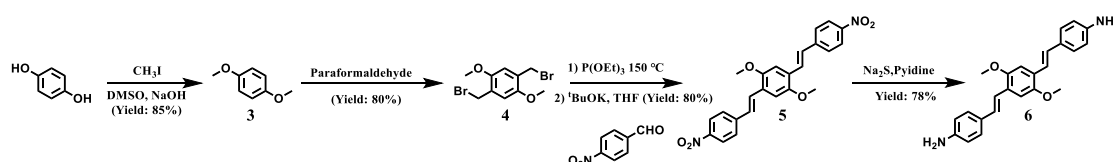


Figure S3. Synthetic routes of compound 2,5-Dimethoxy-1,4-bis(4-aminophenyl)vinyl)benzene (L-OPV-OMe-NH₂).

Compounds were synthesized according to a literature method.²

1,4-Dimethoxybenzene (3)

Hydroquinone (5.5 g, 50 mmol) and NaOH (10 g, 250 mmol) were dissolved in DMSO (50 mL), and stirred while adding CH₃I (7.78 mL, 125 mmol). After adding CH₃I, the reaction was heated at 80 °C for overnight. Then 200 mL water was added to quench and the reaction was stirred and filtered and washed by water to obtain a white powder (5.9022 g, 85% yield). $^1\text{H NMR}$ (400 MHz, Chloroform-d, ppm): $\delta = 6.84$ (s, 4H), 3.77 (s, 6H).

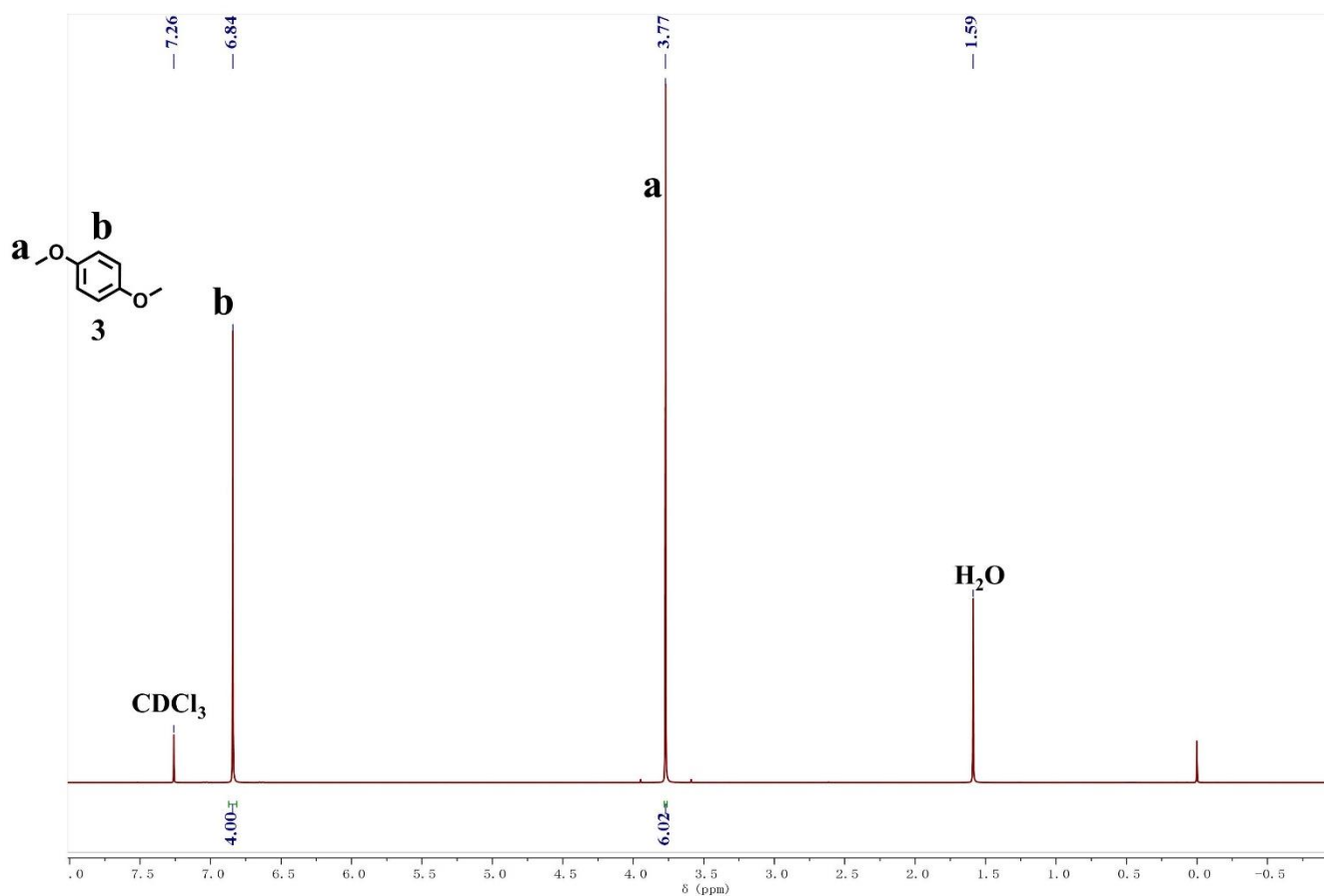


Figure S4. $^1\text{H-NMR}$ spectrum of 1,4-Dimethoxybenzene (3)

1,4-Dimethoxy-2,5-bis(bromomethyl)benzene (4)

Compound 1 (5 g, 36.2 mmol) and Paraformaldehyde (2.3916 g, 79.64 mmol) were dissolved in glacial acetic acid (25.5 mL). After adding 33wt% $\text{HBr}/\text{CH}_3\text{COOH}$ (17 mL) solutions. the reaction was heated at $80\text{ }^\circ\text{C}$ for 4 h under nitrogen atmosphere. Then, the mixture was cooled to room temperature and was poured over 100 mL of ice water. The solid product was filtered and washed by ice water to obtain a white powder (9.3359 g, 80% yield). $^1\text{H NMR}$ (400 MHz, CDCl_3 , ppm): $\delta = 6.88$ (s, 2H), 4.34 (s, 4H), 3.87 (s, 6H).

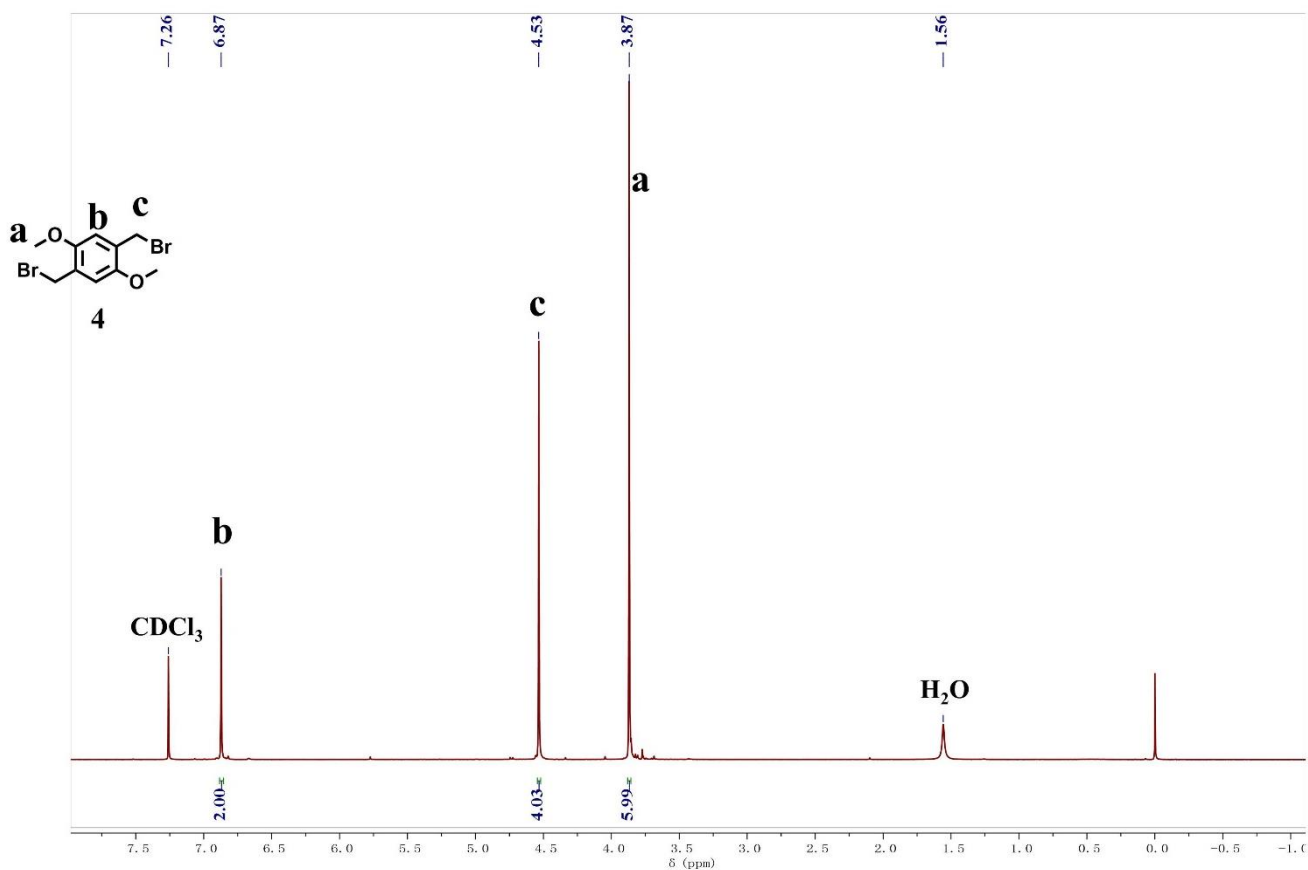


Figure S5. ¹H-NMR spectrum of 1,4-Dimethoxy-2,5-bis(bromomethyl)benzene (4)

2,5-Dimethoxy-1,4-bis(4-nitrophenyl)vinyl)benzene (5)

Compound 2 (0.972 g, 3 mmol) and triethyl phosphite (15 mL, 90 mmol) were added into a 100 mL single mouth bottle under nitrogen atmosphere, and heated at 150 °C for 4 h. After cooling to room temperature, excess triethyl phosphite was removed under reduced pressure, and vacuumed until there are no liquid droplets left at the upper end of the condenser tube, to obtain a white powder. The obtained white powder, THF (30 mL) and 4-nitrobenzaldehyde (1.82 g, 12 mmol) were added into a two necked flask in an ice water bath under nitrogen atmosphere, and the mixture was stirred for 20 min. After adding potassium tert-butoxide (2.02 g, 18 mmol) in batches, the mixture was transferred to room temperature for overnight reaction. Then 50 mL of water was added to quench, 10 mL of 1 M HCl was added to adjust pH to 2~3. After removing the solvent by evaporation, the resulting precipitate was filtered. The solid residue was washed by water, methanol and dichloromethane to afford a dark red powder (1.02 g, 80% yield). The obtained dark red solid is insoluble in chloroform and DMSO, and can be put into the next reaction

without further purification.

2,5- Dimethoxy-1,4-bis(4-aminophenyl)vinyl)benzene (6)

Compound 3 (1.02 g, 2.36 mmol) was dissolved in 10 mL of pyridine and taken to ebullition. Then, a solution of Na₂S 9H₂O (3.41 g, 14.19 mmol) in 10 mL of water was added while maintaining a gentle reflux. At this point, the color of the reaction mixture changes to dark brown. After the addition is complete, the reaction was stirred and heated at 115 °C for 30 additional minutes. Then, the crude was poured over 100 mL of cold water. The solid product was filtered and washed by water to obtain a reddish brown powder (0.6858 g, 78% yield). ¹H NMR (400 MHz, Chloroform-d, ppm): δ = 7.39 (d, 4H), 7.31 (d, 2H), 7.09 (d, 2H), 6.99 (d, 2H), 6.69 (d, 4H), 3.90 (s, 6H), 3.74 (s, 4H).

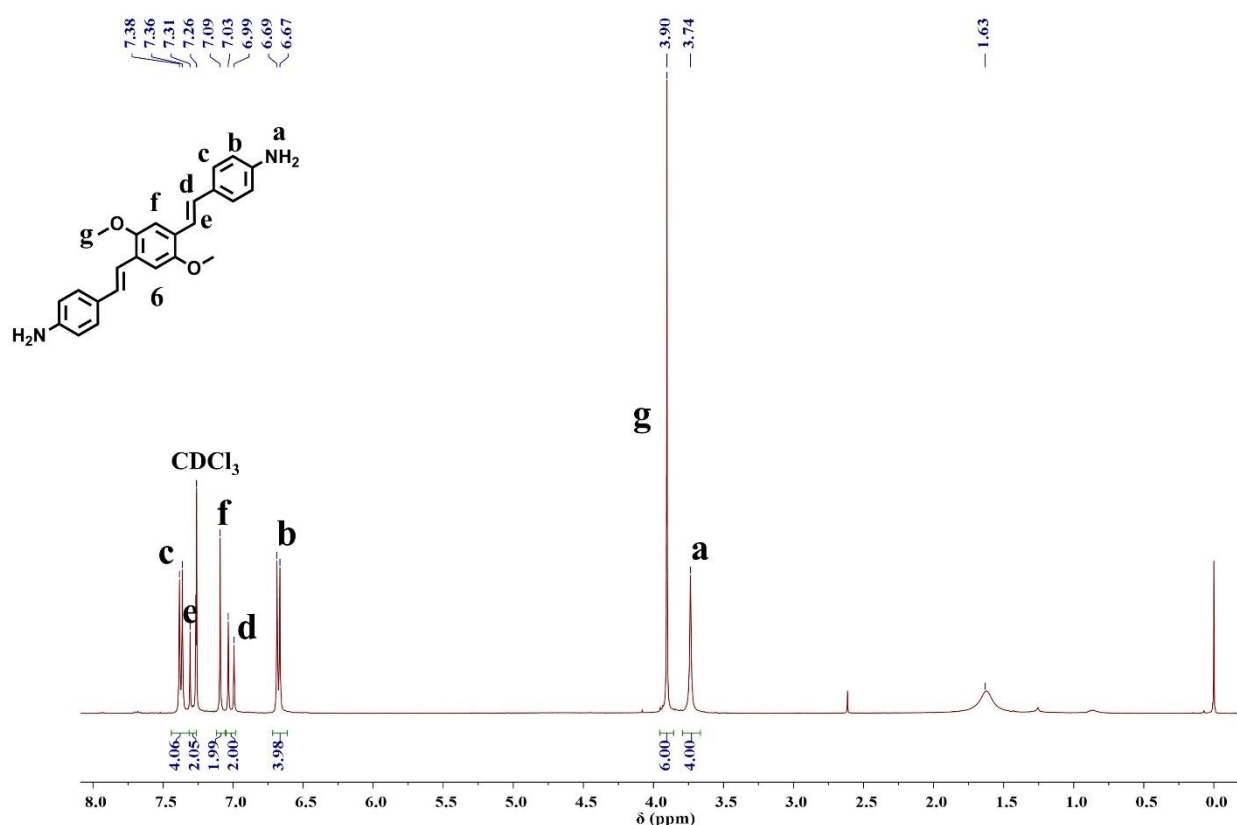


Figure S6. ¹H-NMR spectrum of 2,5- Dimethoxy-1,4-bis(4-aminophenyl)vinyl)benzene (6)

Synthesis of 1,3,5-triformylbenzene (TFB)

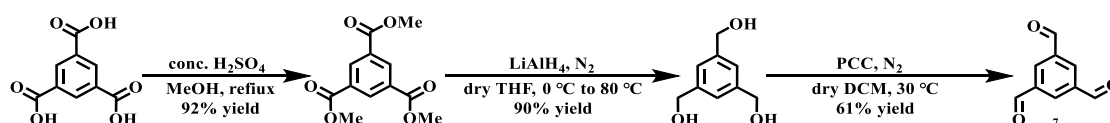


Figure S7. Synthetic routes of 1,3,5-triformylbenzene (TFB)

Compound 7 was synthesized according to a literature method³. ¹H NMR (400 MHz, 298 K, CDCl₃, ppm): δ = 10.21 (s, 3H), 8.64 (s, 3H).

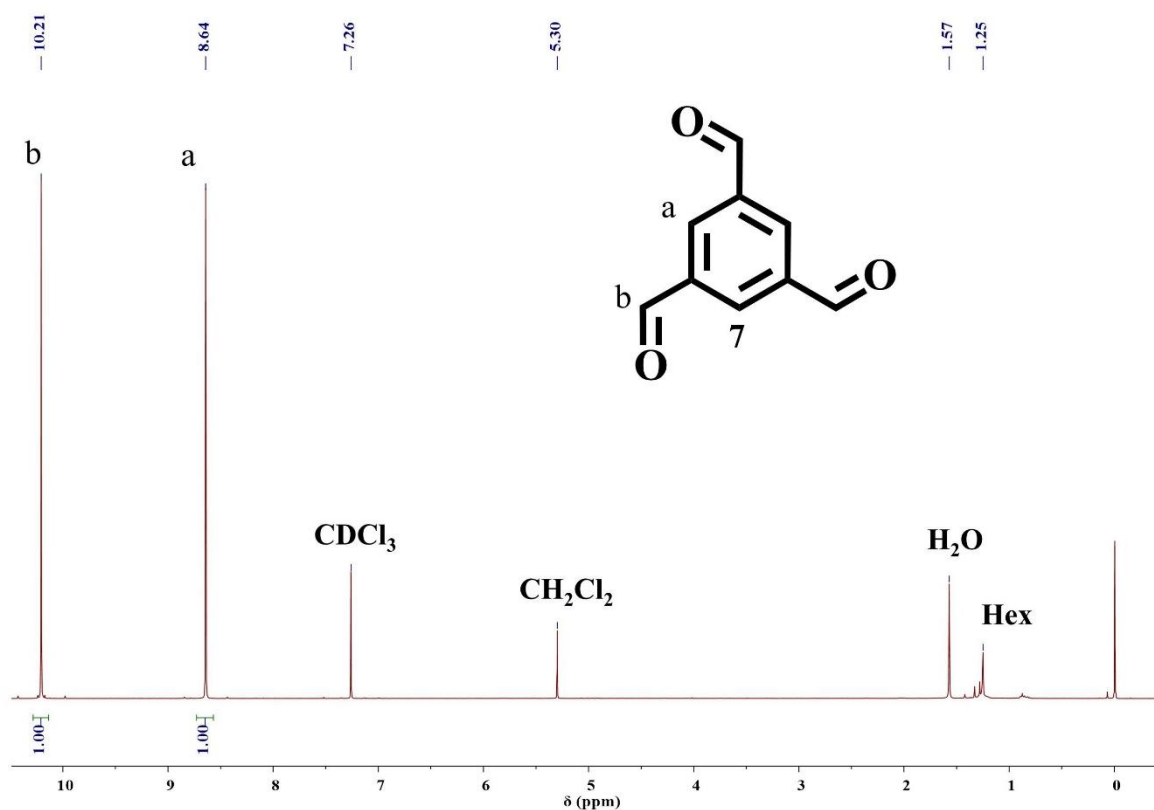


Figure S8. ¹H-NMR spectrum of TFB (7)

Synthesis of 2,4,6-triformylresorcinol (TFR)

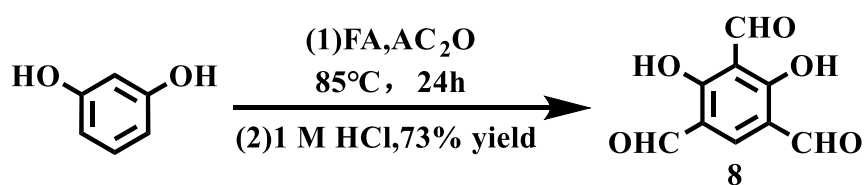


Figure S9. Synthetic routes of 2,4,6-triformylresorcinol (TFR)

Compound 8 was synthesized according to a literature method⁴. ¹H NMR (400 MHz, DMSO-d₆) δ = 10.26 (s, 1H), 10.09 (s, 2H), 8.39 (s, 1H).

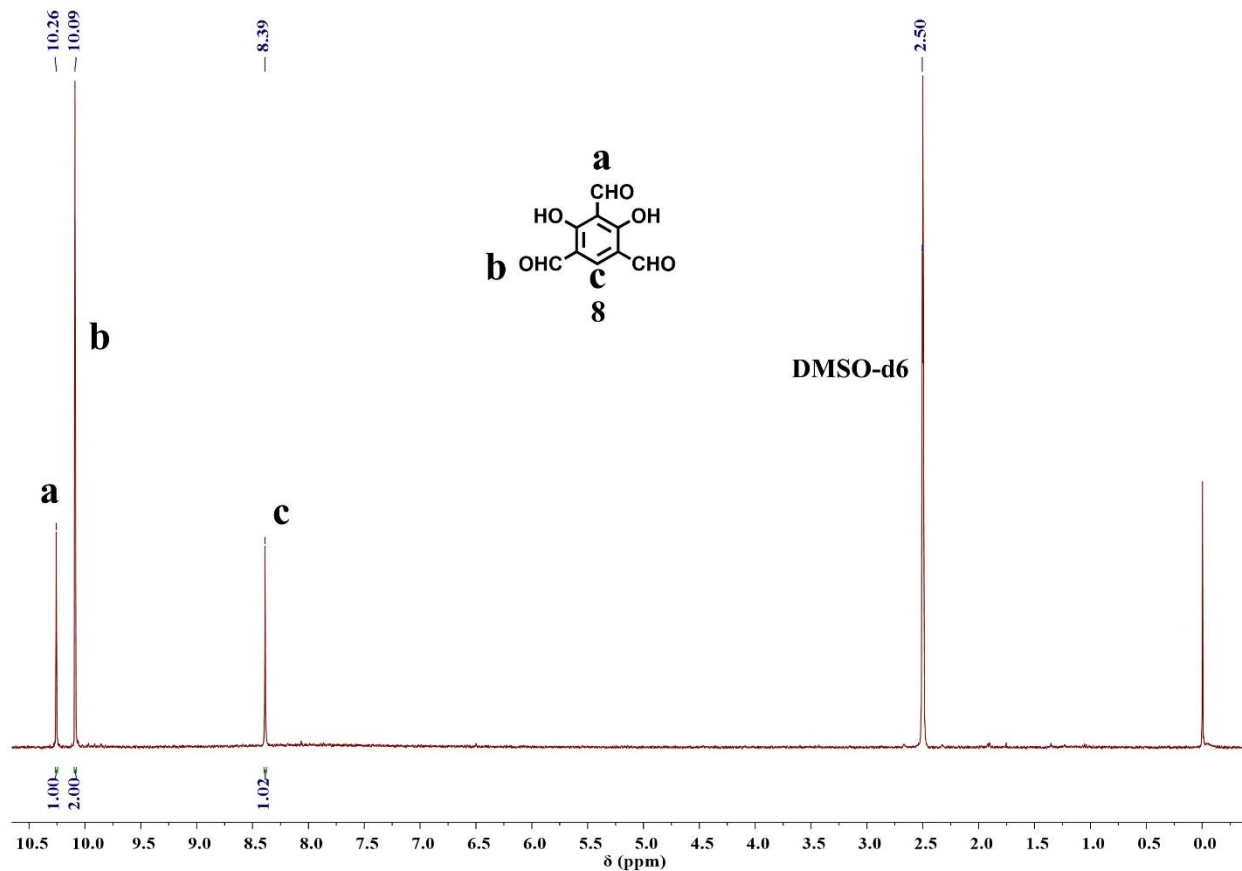


Figure S10. $^1\text{H-NMR}$ spectrum of TFR (8)

Synthesis of 1,3,5-triformylphloroglucinol (Tp)

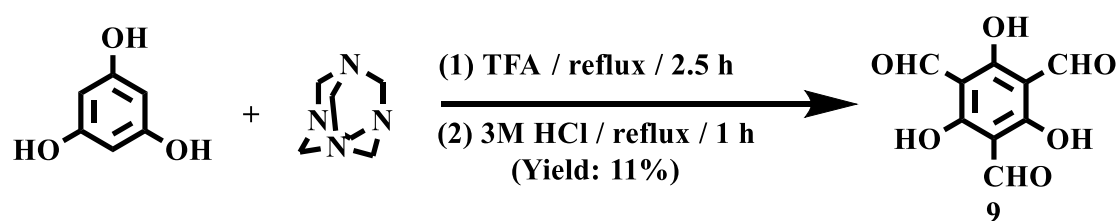


Figure S11. Synthetic routes of 1,3,5-triformylphloroglucinol (Tp)

Compound 9 was synthesized according to a literature method⁵. $^1\text{H NMR}$ (400 MHz, Chloroform-d) δ 14.12 (s, 3H), 10.15 (s, 3H). $^{13}\text{C NMR}$ (101 MHz, Chloroform-d) δ 192.21, 173.74, 103.03.

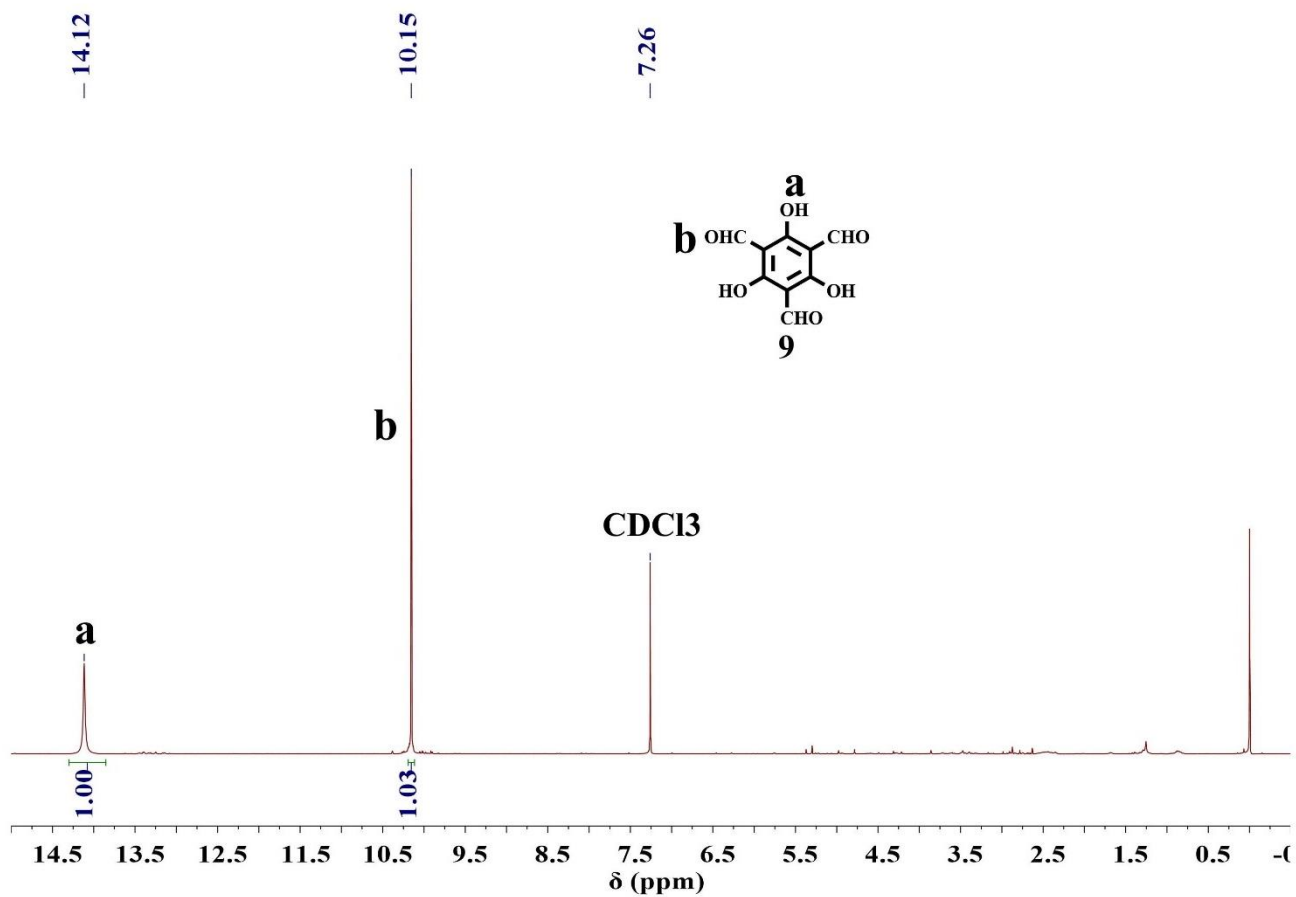


Figure S12. $^1\text{H-NMR}$ spectrum of Tp (**9**)

Synthesis of COF-950-TFB

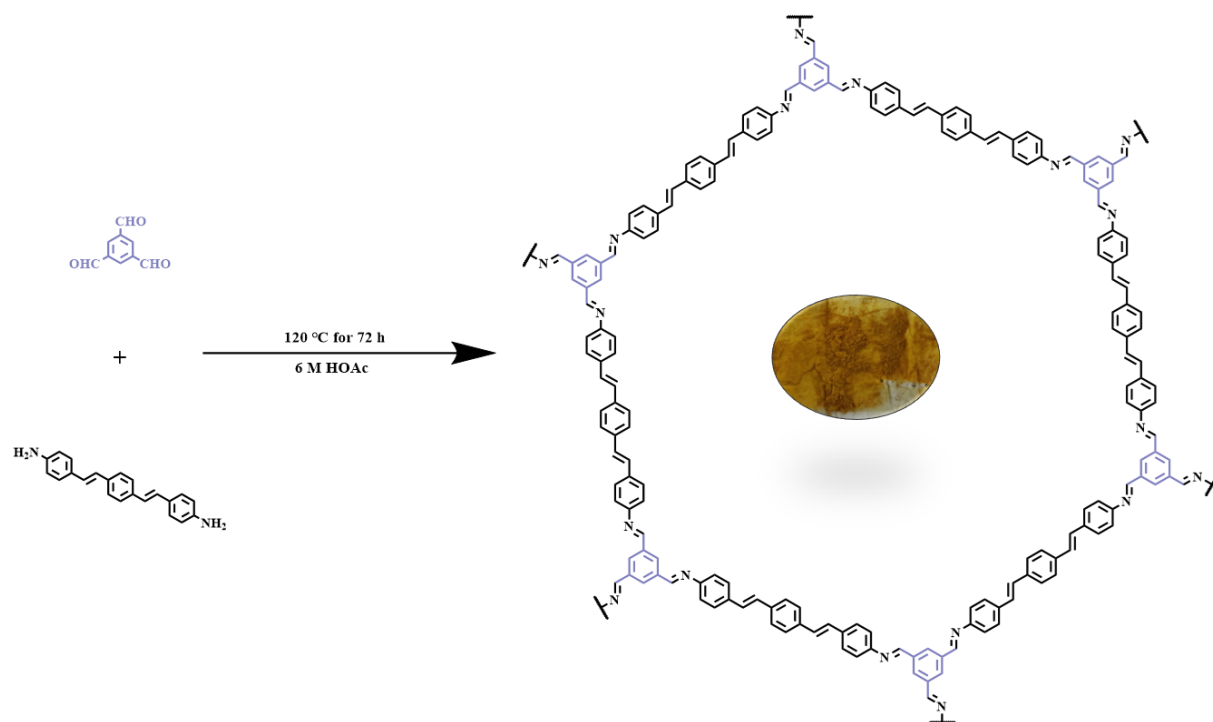


Figure S13. Synthetic routes of COF-950-TFB

L-OPV-NH₂ (23.1 mg, 0.074 mmol) and TFB (8.1 mg, 0.05 mmol) were added into a glass tube, then the mixture was dissolved in reaction solution (mesitylene/dioxane, v/v = 0.75 mL/0.25 mL, 0.5 mL/0.5 mL, 0.25 mL/0.75 mL, o-dichlorobenzene/n-butanol, v/v = 0.75 mL/0.25 mL, 0.5 mL/0.5 mL, 0.25 mL/0.75 mL), which were used to explore the best synthesis condition. The mixture was added 0.1 mL (6 M) HOAc aqueous solution. Then the tube was flash frozen in a liquid nitrogen bath and flame sealed degassed through three freeze-pump-thaw cycles and sealed under vacuum. Upon warming to room temperature, the ampoule was placed in an oven at 120 °C and left undisturbed for 3 days. The resulting precipitate was filtered, exhaustively washed by methanol. The resulting solid was dried, and then subjected to Soxhlet extractions with THF and acetone for 1 day, respectively, to remove the trapped guest molecules. The solid was washed by methanol for 12 h and then dried by supercritical CO₂. The powder was collected and dried under vacuum condition at 120 °C for 12 h to yield COF-950-TFB as a yellow powder (14.9 mg, yield 52% in condition with Mes/Dio= 1:3).

Synthesis of COF-950-TFR

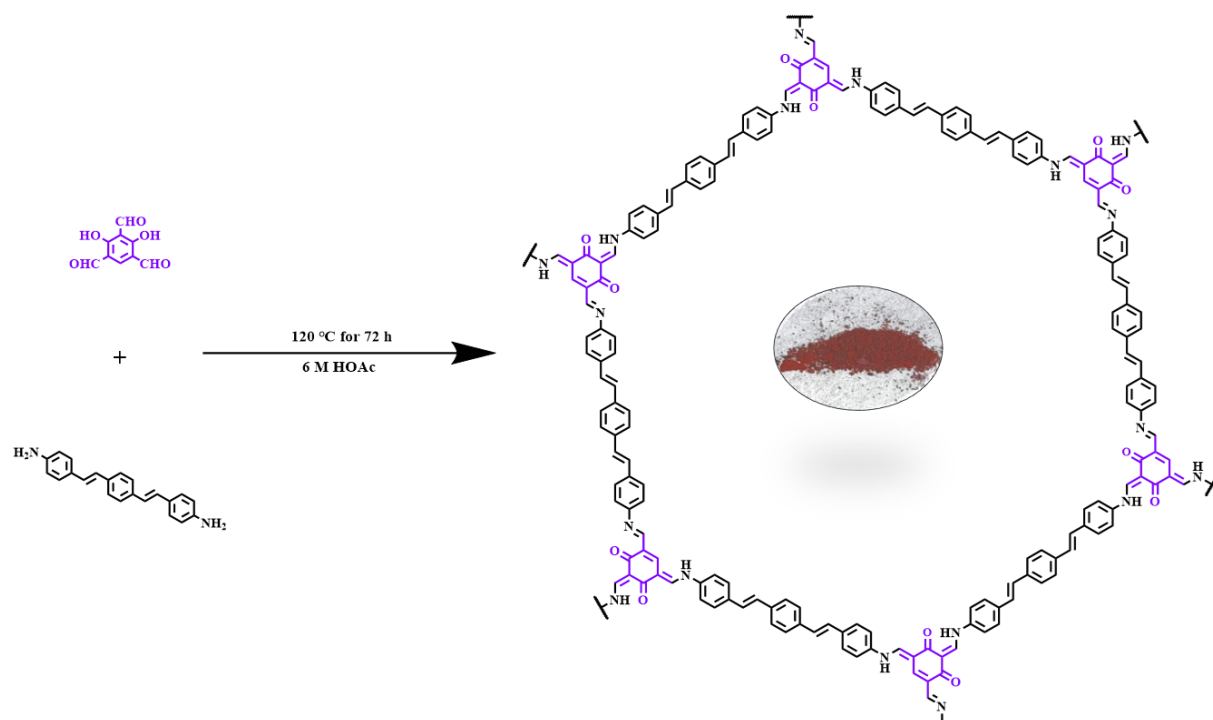


Figure S14. Synthetic routes of COF-950-TFR

L-OPV-NH₂ (23.1 mg, 0.074 mmol) and TFR (9.5 mg, 0.05 mmol) were added into a glass tube, then the mixture was dissolved in reaction solution (mesitylene/dioxane, v/v = 0.75 mL/0.25 mL, 0.5 mL/0.5 mL, 0.25 mL/0.75 mL, o-dichlorobenzene/n-butanol, v/v = 0.75 mL/0.25 mL, 0.5 mL/0.5 mL, 0.25 mL/0.75 mL), which were used to explore the best synthesis condition. The mixture was added 0.1 mL (6 M) HOAc aqueous solution. Then the tube was flash frozen in a liquid nitrogen bath and flame sealed degassed through three freeze-pump-thaw cycles and sealed under vacuum. Upon warming to room temperature, the ampoule was placed in an oven at 120 °C and left undisturbed for 3 days. The resulting precipitate was filtered, exhaustively washed by methanol. The resulting solid was dried, and then subjected to Soxhlet extractions with THF and acetone for 1 day, respectively, to remove the trapped guest molecules. The solid was washed by methanol for 12 h and then dried by supercritical CO₂. The powder was collected and dried under vacuum condition at 120 °C for 12 h to yield COF-950-TFR as a dark powder (11.4 mg, yield 38% in condition with Mes/Dio = 1:3).

Synthesis of COF-950-Tp

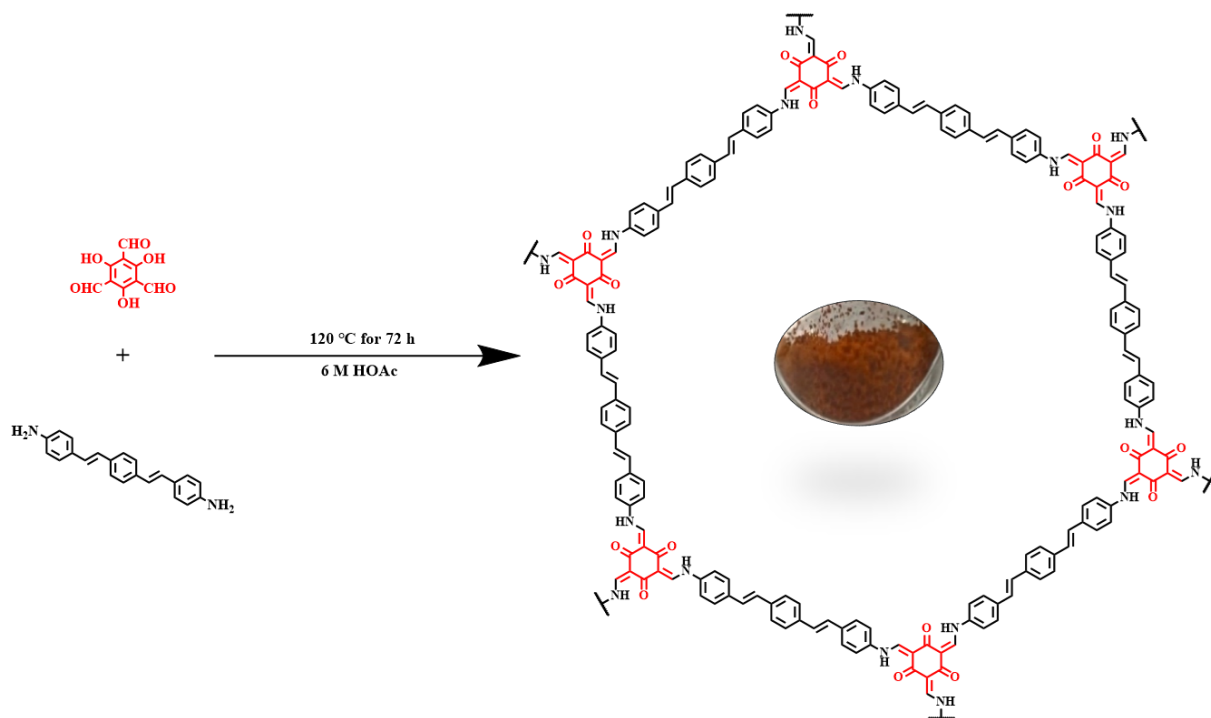


Figure S15. Synthetic routes of COF-950-Tp

L-OPV-NH₂ (23.1 mg, 0.074 mmol) and Tp (10.4 mg, 0.05 mmol) were added into a glass tube, then the mixture was dissolved in reaction solution (mesitylene/dioxane, v/v = 0.75 mL/0.25 mL, 0.5 mL/0.5 mL, 0.25 mL/0.75 mL, o-dichlorobenzene/n-butanol, v/v = 0.75 mL/0.25 mL, 0.5 mL/0.5 mL, 0.25 mL/0.75 mL), which were used to explore the best synthesis condition. The mixture was added 0.1 mL (6 M) HOAc aqueous solution. Then the tube was flash frozen in a liquid nitrogen bath and flame sealed degassed through three freeze-pump-thaw cycles and sealed under vacuum. Upon warming to room temperature, the ampoule was placed in an oven at 120 °C and left undisturbed for 3 days. The resulting precipitate was filtered, exhaustively washed by methanol. The resulting solid was dried, and then subjected to Soxhlet extractions with THF and acetone for 1 day, respectively, to remove the trapped guest molecules. The solid was washed by methanol for 12 h and then dried by supercritical CO₂. The powder was collected and dried under vacuum condition at 120 °C for 12 h to yield COF-950-Tp as a red powder (23.1 mg, yield 74% in condition with o-DCB/n-BuOH = 1:1).

Synthesis of COF-950-OMe-TFB

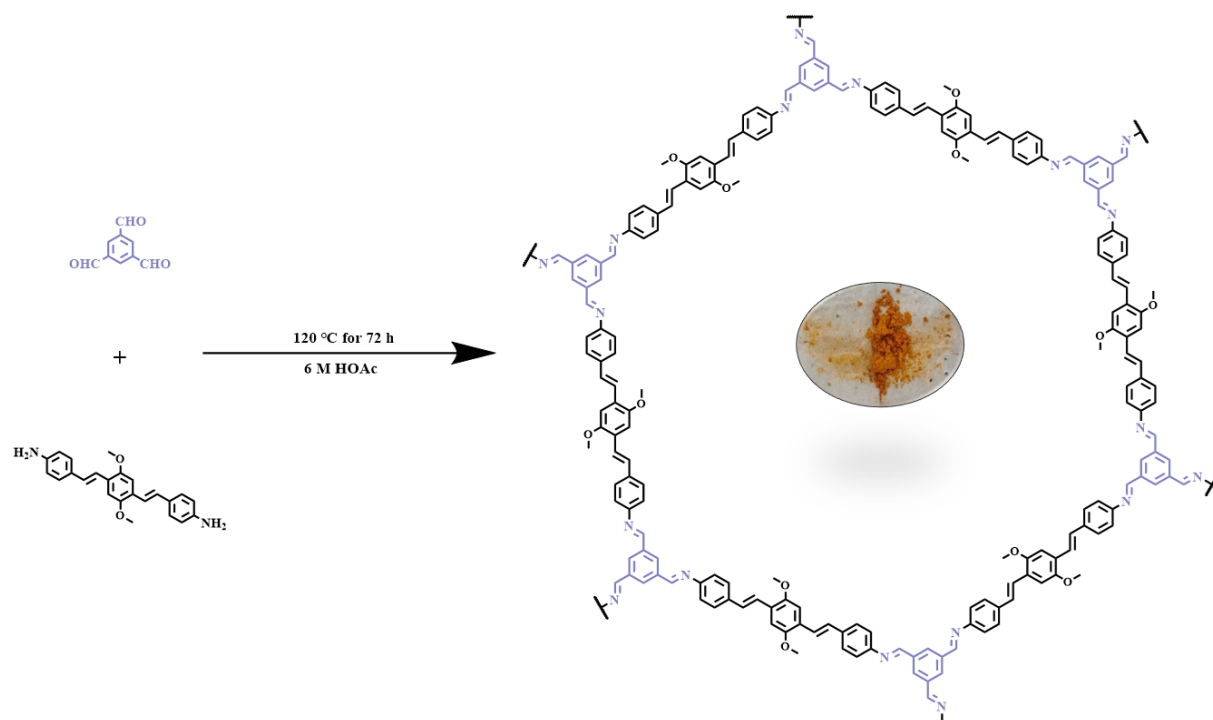


Figure S16. Synthetic routes of COF-950-OMe-TFB

L-OPV-OMe-NH₂ (24.1 mg, 0.065 mmol) and TFB (7.5 mg, 0.043 mmol) were added into a glass tube, then the mixture was dissolved in reaction solution (mesitylene/dioxane, v/v = 0.75 mL/0.25 mL, 0.5 mL /0.5 mL, 0.25 mL /0.75 mL, o-dichlorobenzene/n-butanol, v/v = 0.75 mL/0.25 mL, 0.5 mL /0.5 mL, 0.25 mL /0.75 mL), which were used to explore the best synthesis condition. the mixture was added 0.1 mL (6 M) HOAc aqueous solution. Then the tube was flash frozen in a liquid nitrogen bath and flame sealed degassed through three freeze-pump-thaw cycles and sealed under vacuum. Upon warming to room temperature, the ampoule was placed in an oven at 120 °C and left undisturbed for 3 days. The resulting precipitate was filtered, exhaustively washed by methanol. The resulting solid was dried, and then subjected to Soxhlet extractions with THF and acetone for 1 day, respectively, to remove the trapped guest molecules. The solid was washed by methanol for 12 h and then dried by supercritical CO₂. The powder was collected and dried under vacuum condition at 120 °C for 12 h to yield COF-950-OMe-TFB as a yellow powder (21.0 mg, yield 73% in condition with o-DCB/n-BuOH= 3:1).

Synthesis of COF-950-OMe-TFR

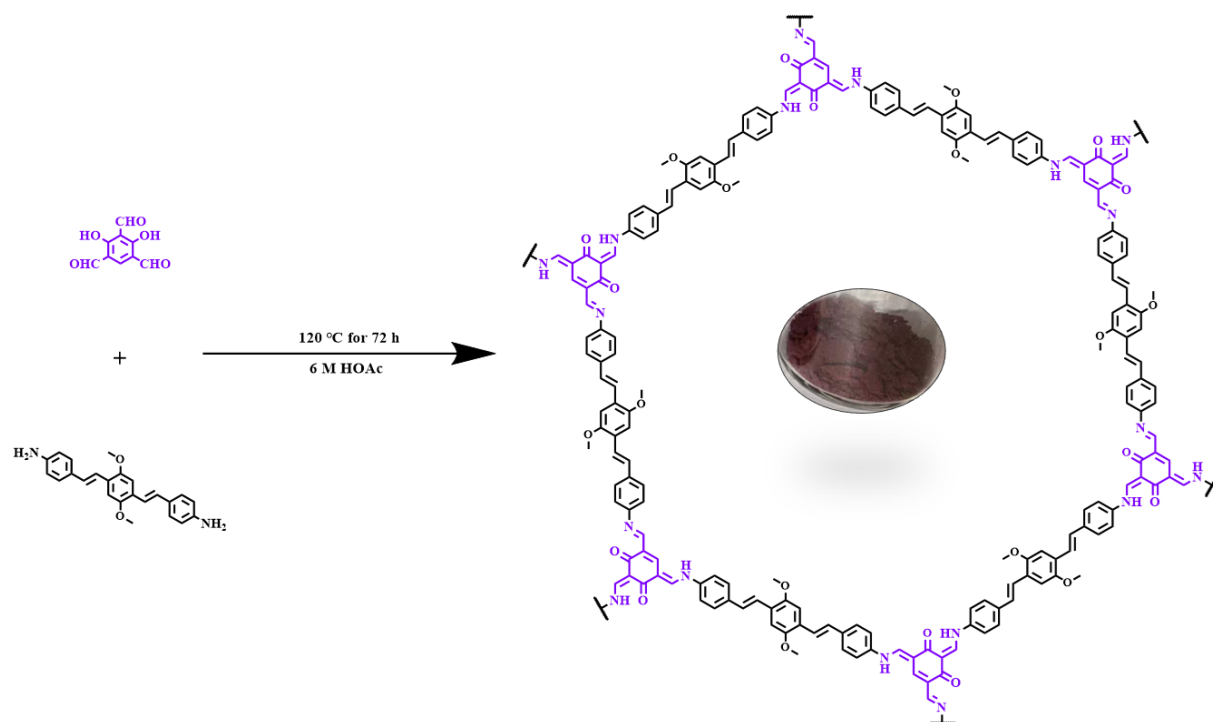


Figure S17. Synthetic routes of COF-950-OMe-TFR

L-OPV-OMe-NH₂ (24.1 mg, 0.065 mmol) and TFR (8.4 mg, 0.043 mmol) were added into a glass tube, then the mixture was dissolved in reaction solution (mesitylene/dioxane, v/v = 0.75 mL/0.25 mL, 0.5 mL /0.5 mL, 0.25 mL /0.75 mL, o-dichlorobenzene/n-butanol, v/v = 0.75 mL/0.25 mL, 0.5 mL /0.5 mL, 0.25 mL /0.75 mL), which were used to explore the best synthesis condition. the mixture was added 0.1 mL (6 M) HOAc aqueous solution. Then the tube was flash frozen in a liquid nitrogen bath and flame sealed degassed through three freeze-pump-thaw cycles and sealed under vacuum. Upon warming to room temperature, the ampoule was placed in an oven at 120 °C and left undisturbed for 3 days. The resulting precipitate was filtered, exhaustively washed by methanol. The resulting solid was dried, and then subjected to Soxhlet extractions with THF and acetone for 1 day, respectively, to remove the trapped guest molecules. The solid was washed by methanol for 12 h and then dried by supercritical CO₂. The powder was collected and dried under vacuum condition at 120 °C for 12 h to yield COF-950-OMe-TFR as a dark powder (20.7 mg, yield 69% in condition with o-DCB/n-BuOH= 1:3).

Synthesis of COF-950-OMe-Tp

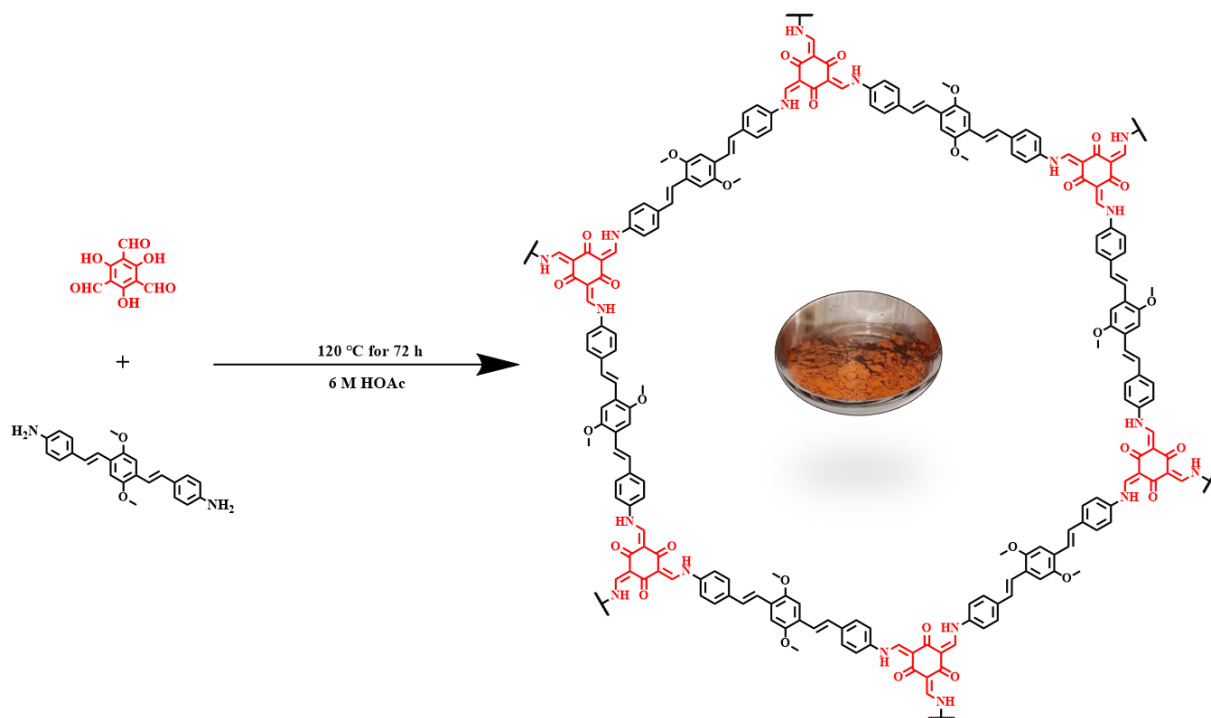


Figure S18. Synthetic routes of COF-950-OMe-Tp

L-OPV-OMe-NH₂ (24.1 mg, 0.065 mmol) and Tp (9.1 mg, 0.043 mmol) were added into a glass tube, then the mixture was dissolved in reaction solution (mesitylene/dioxane, v/v = 0.75 mL/0.25 mL, 0.5 mL /0.5 mL, 0.25 mL /0.75 mL, o-dichlorobenzene/n-butanol, v/v = 0.75 mL/0.25 mL, 0.5 mL /0.5 mL, 0.25 mL /0.75 mL), which were used to explore the best synthesis condition. the mixture was added 0.1 mL (6 M) HOAc aqueous solution. Then the tube was flash frozen in a liquid nitrogen bath and flame sealed degassed through three freeze-pump-thaw cycles and sealed under vacuum. Upon warming to room temperature, the ampoule was placed in an oven at 120 °C and left undisturbed for 3 days. The resulting precipitate was filtered, exhaustively washed by methanol. The resulting solid was dried, and then subjected to Soxhlet extractions with THF and acetone for 1 day, respectively, to remove the trapped guest molecules. The solid was washed by methanol for 12 h and then dried by supercritical CO₂. The powder was collected and dried under vacuum condition at 120 °C for 12 h to yield COF-950-OMe-Tp as a red powder (25.8 mg, yield 84% in condition with o-DCB/n-BuOH= 1:3).

Section S3. Characterization data

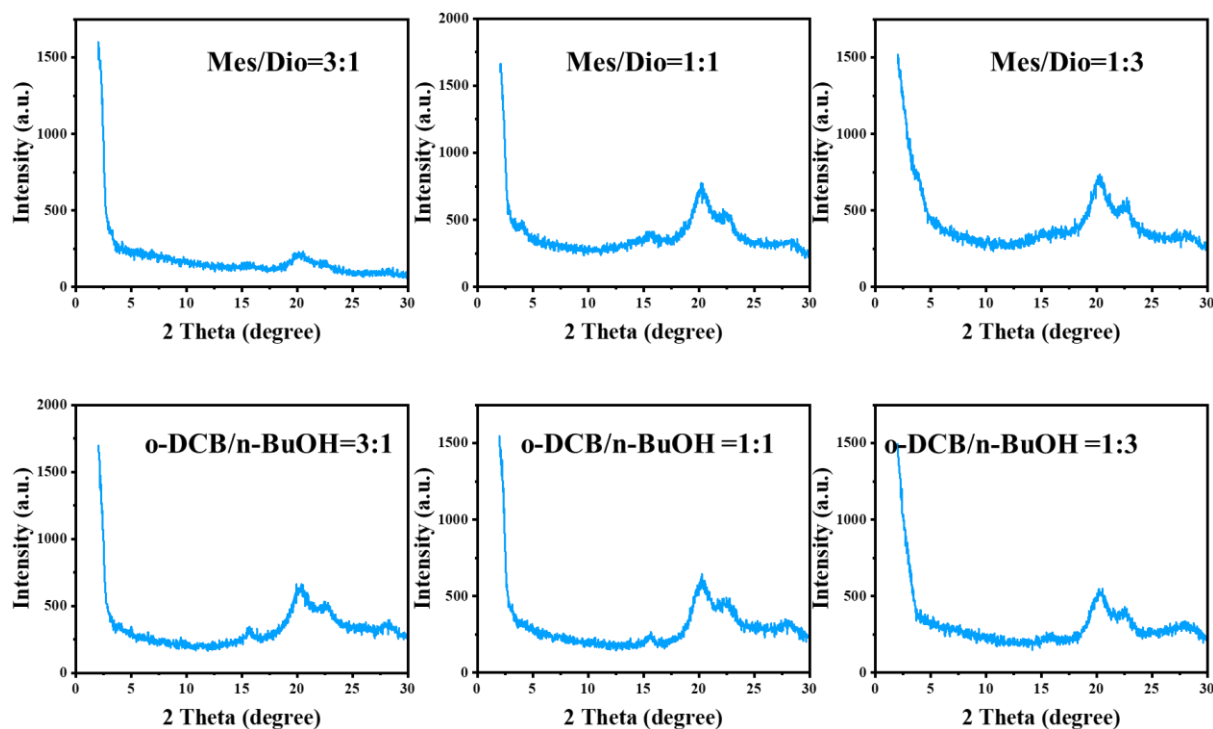


Figure S19. PXR D of COF-950-TFB synthesized in different reaction solution

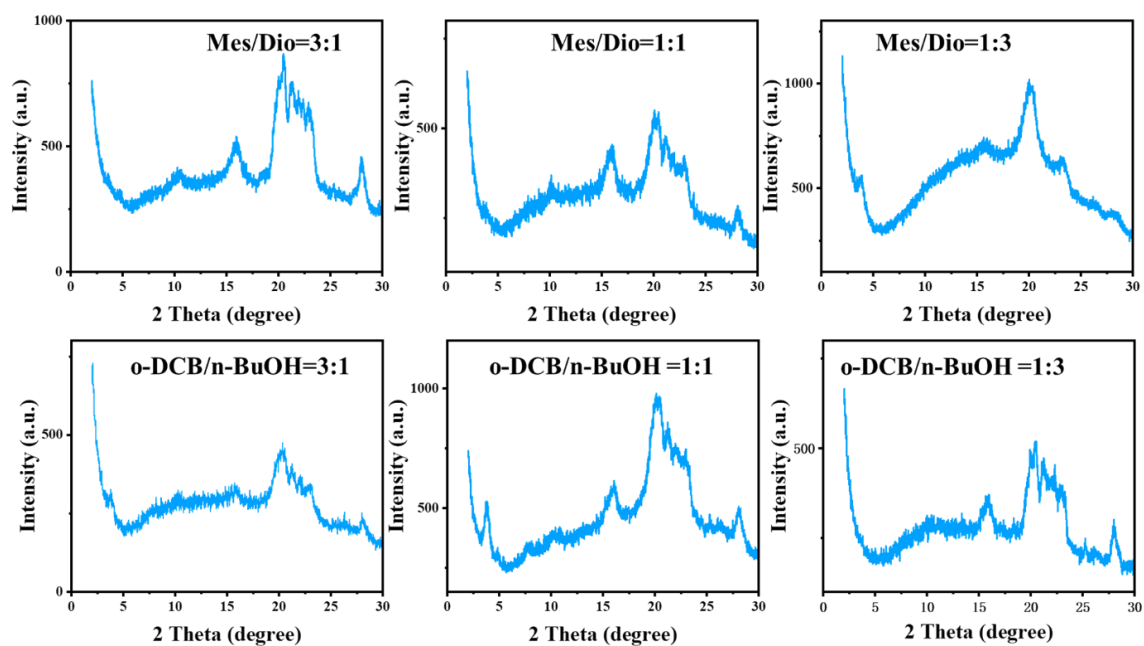


Figure S20. PXR D of COF-950-TFR synthesized in different reaction solution

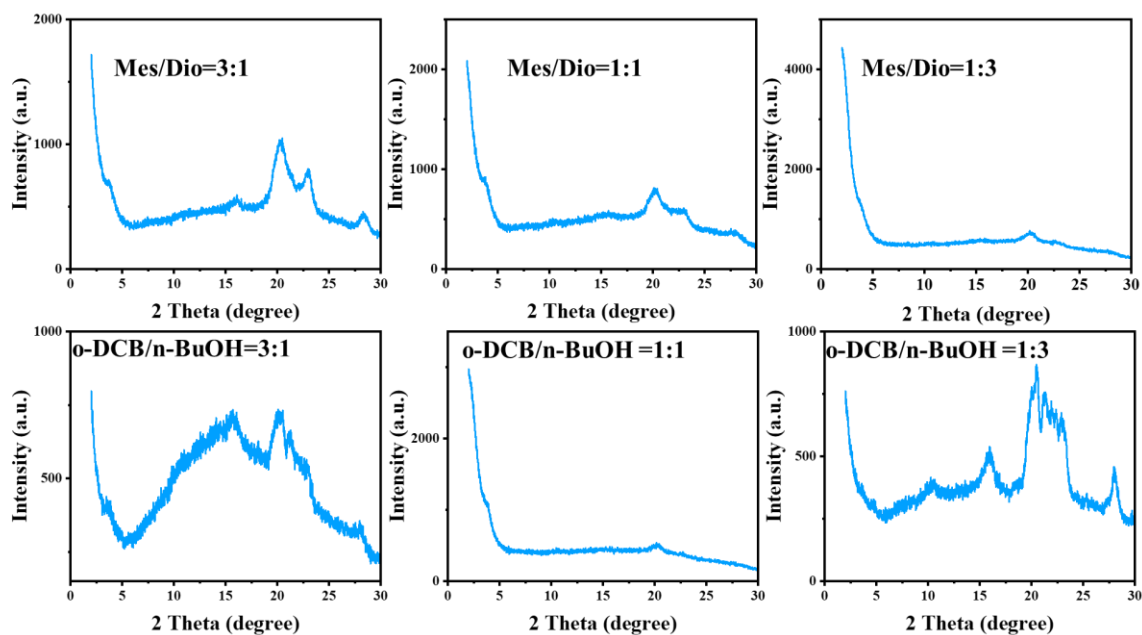


Figure S21. PXRD of COF-950-Tp synthesized in different reaction solution

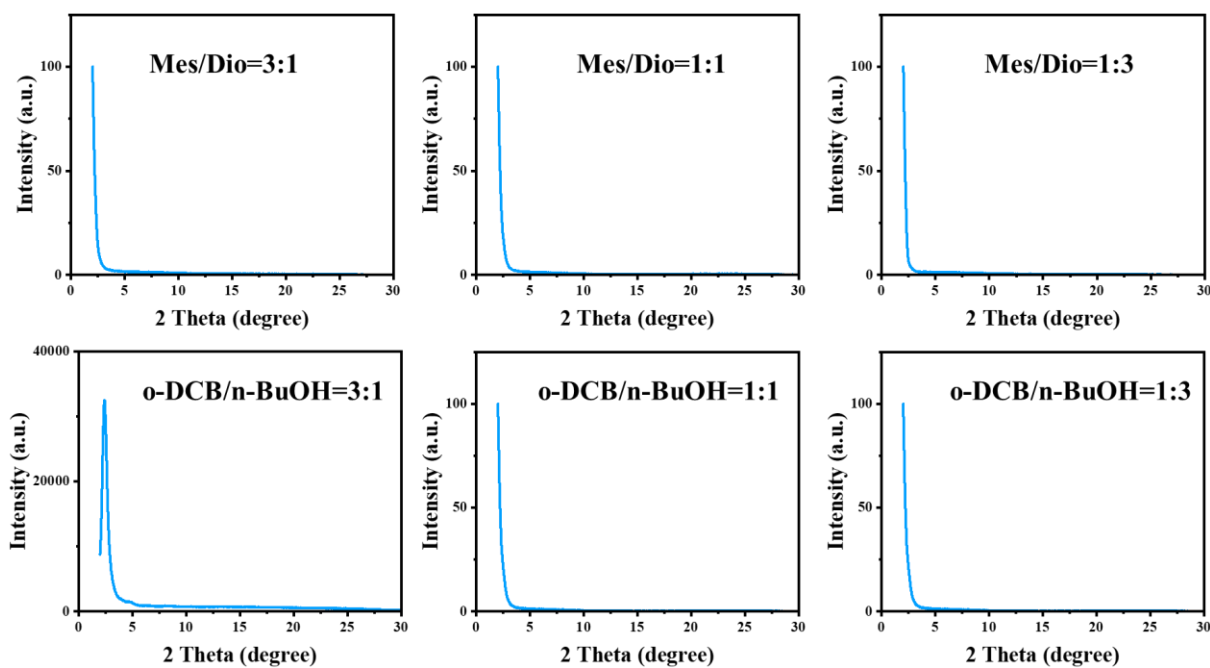


Figure S22. PXRD of COF-950-OMe-TFB synthesized in different reaction solution

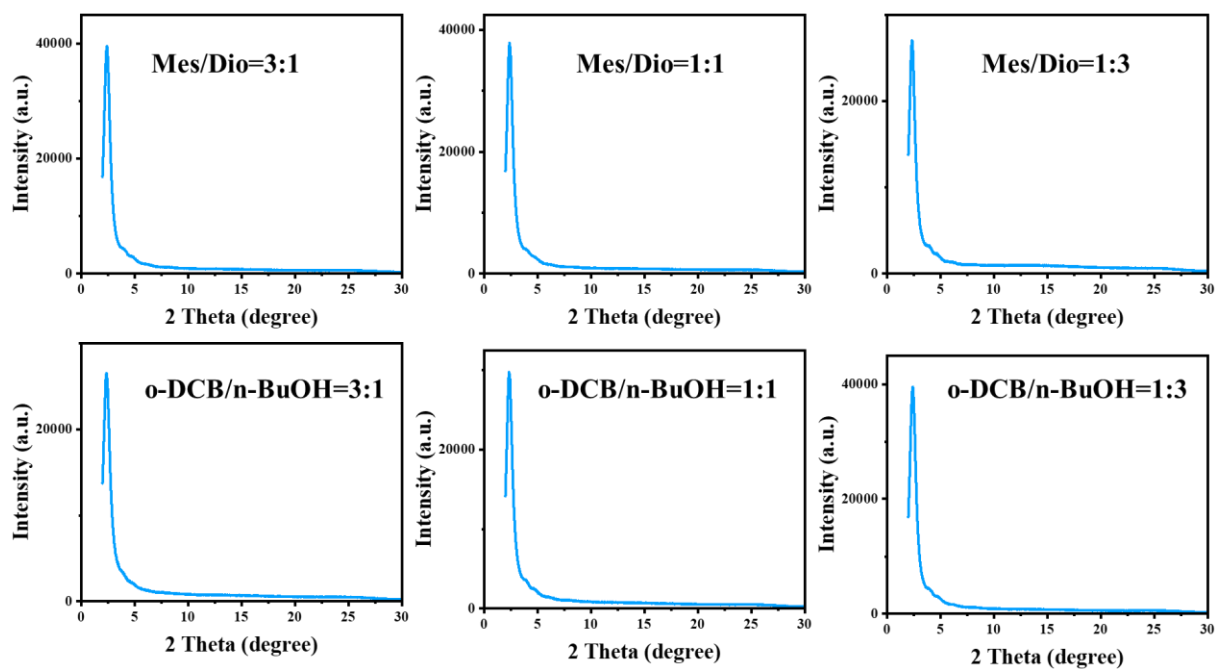


Figure S23. PXRD of COF-950-OMe-TFR synthesized in different reaction solution

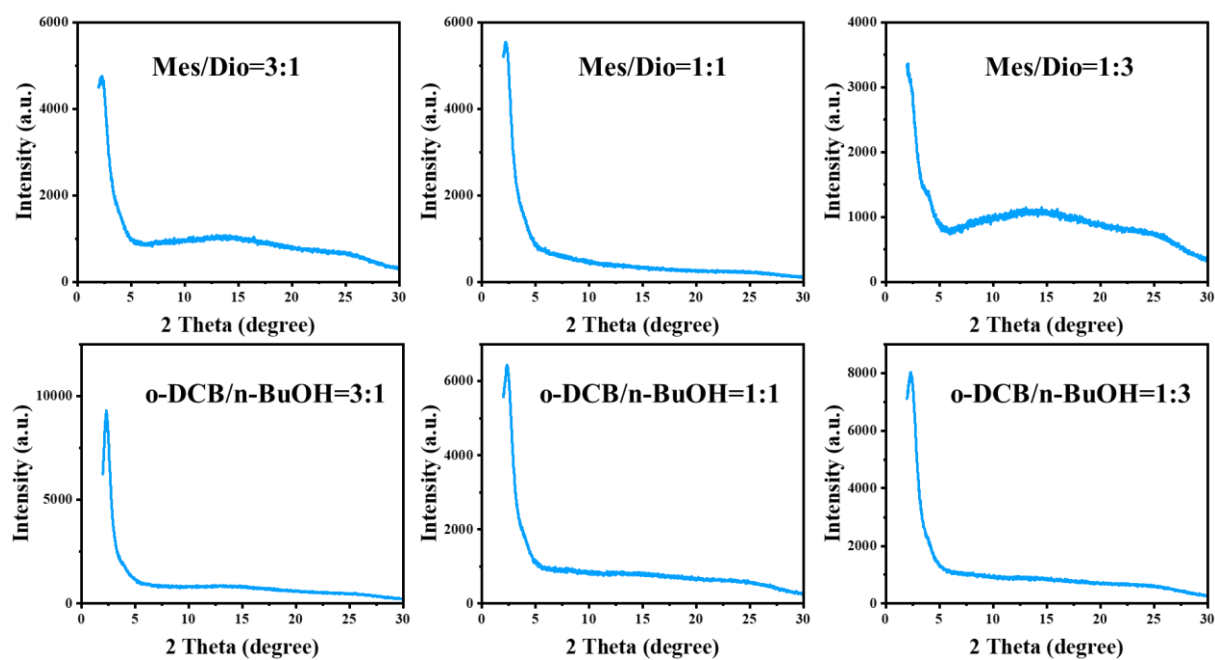


Figure S24. PXRD of COF-950-OMe-Tp synthesized in different reaction solution

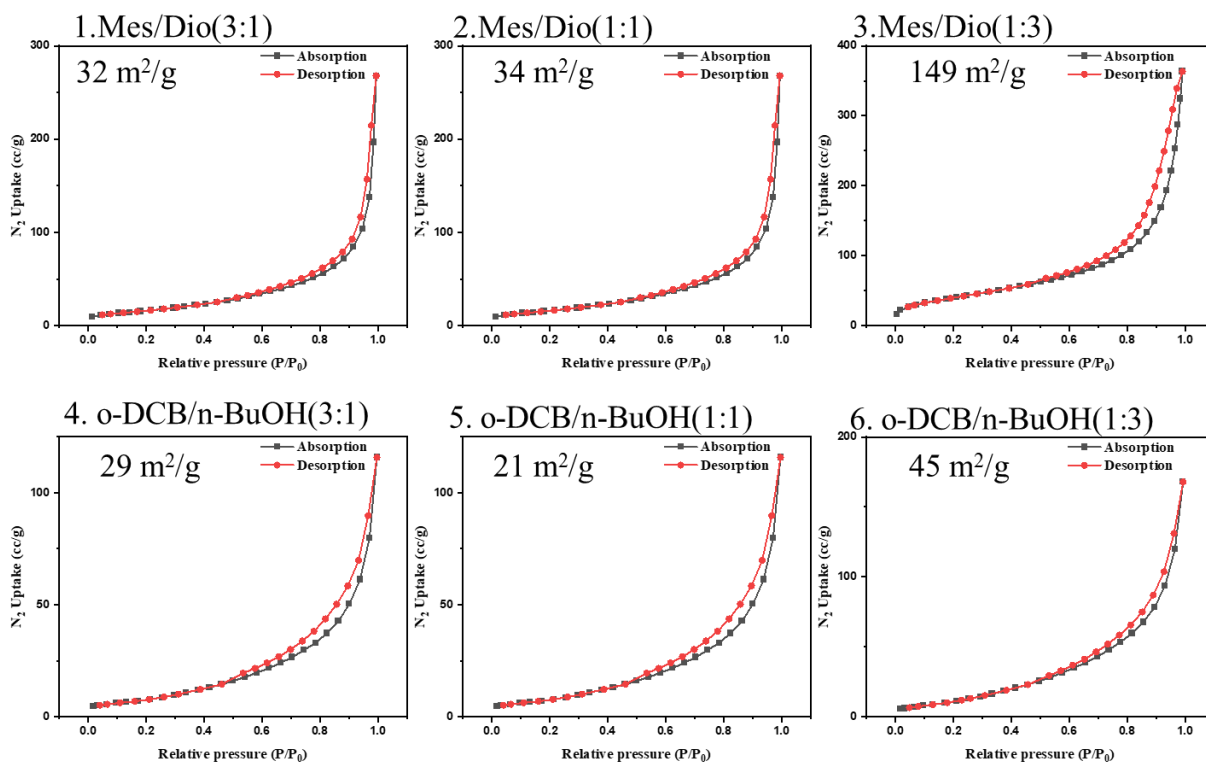


Figure S25. N_2 adsorption-desorption isotherms of COF-950-TFB synthesized in different reaction solution

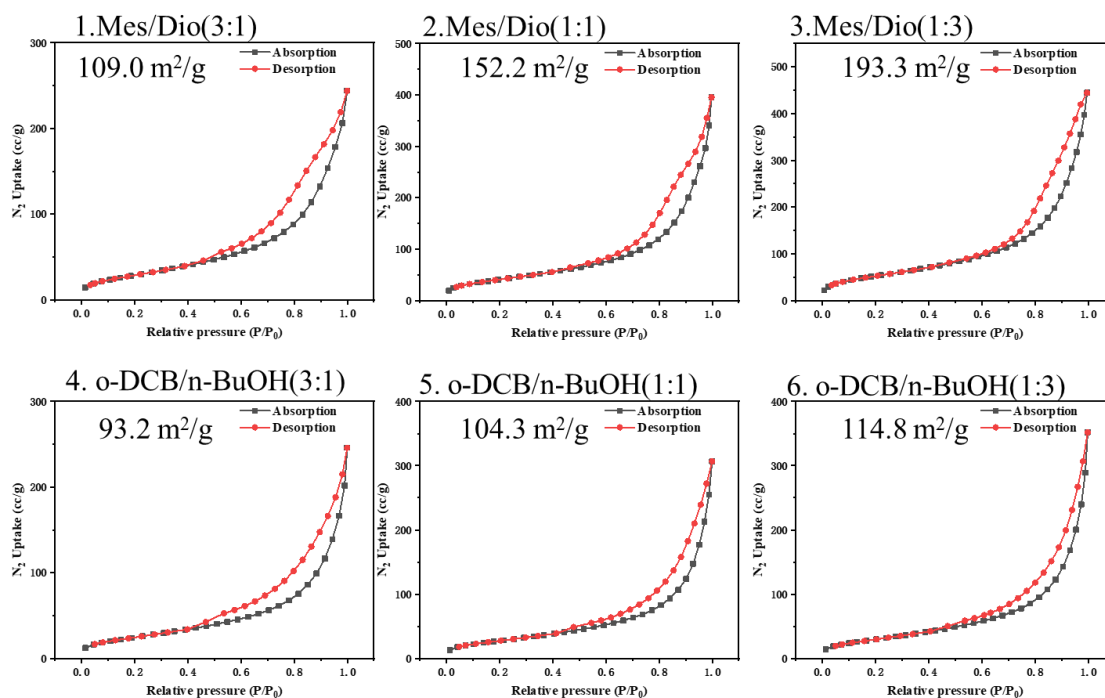


Figure S26. N_2 adsorption-desorption isotherms of COF-950-TFR synthesized in different reaction solution

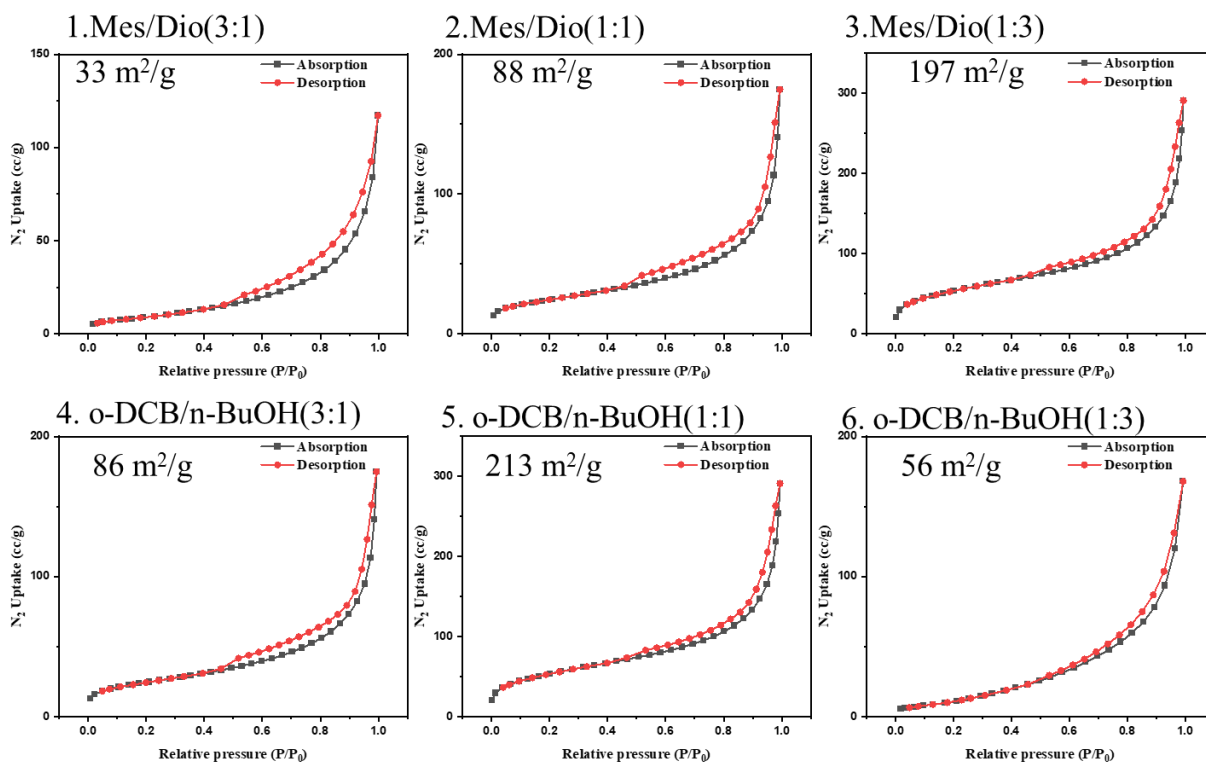


Figure S27. N₂ adsorption-desorption isotherms of COF-950-Tp synthesized in different reaction solution

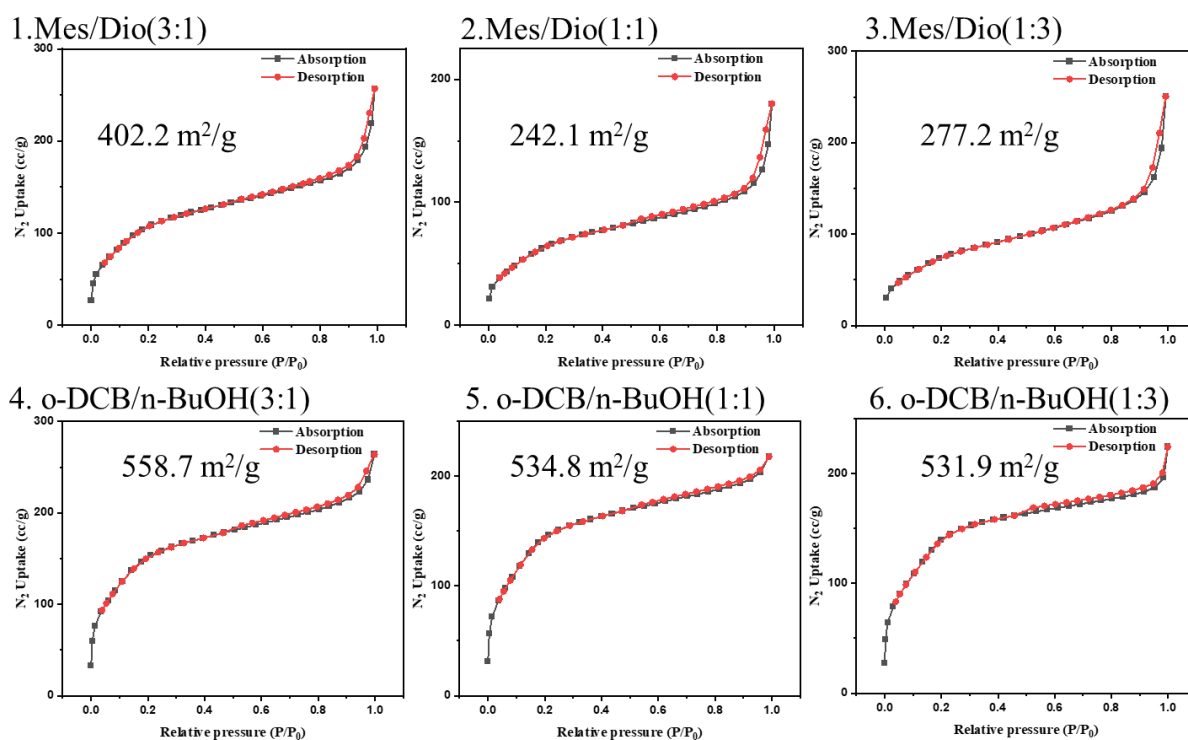


Figure S28. N₂ adsorption-desorption isotherms of COF-950-OMe-TFB synthesized in different reaction solution

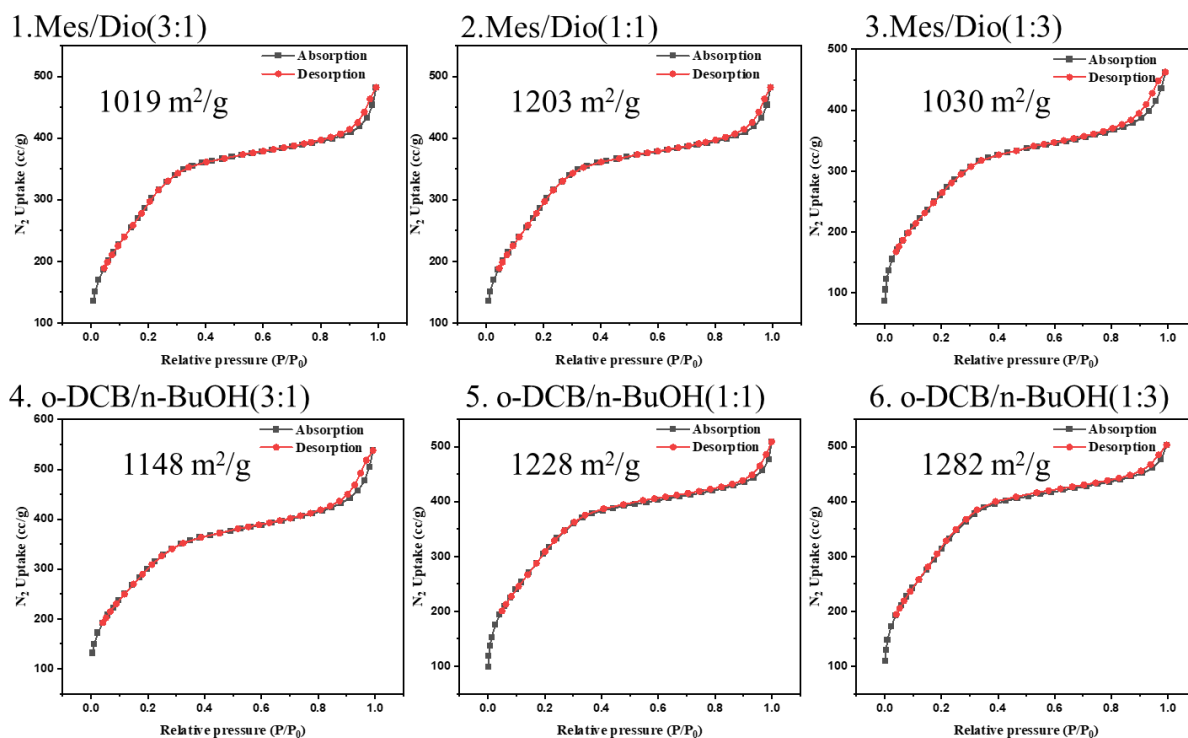


Figure S29. N₂ adsorption-desorption isotherms of COF-950-OMe-TFR synthesized in different reaction solution

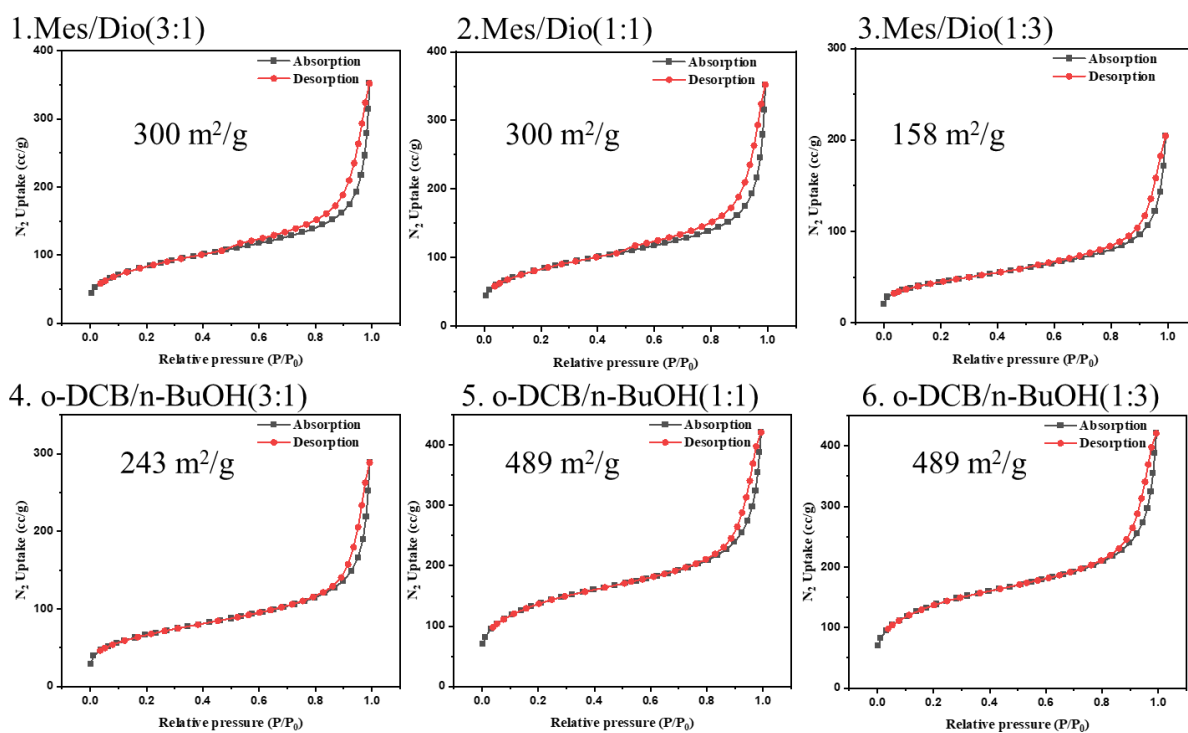


Figure S30. N₂ adsorption-desorption isotherms of COF-950-OMe-Tp synthesized in different reaction solution

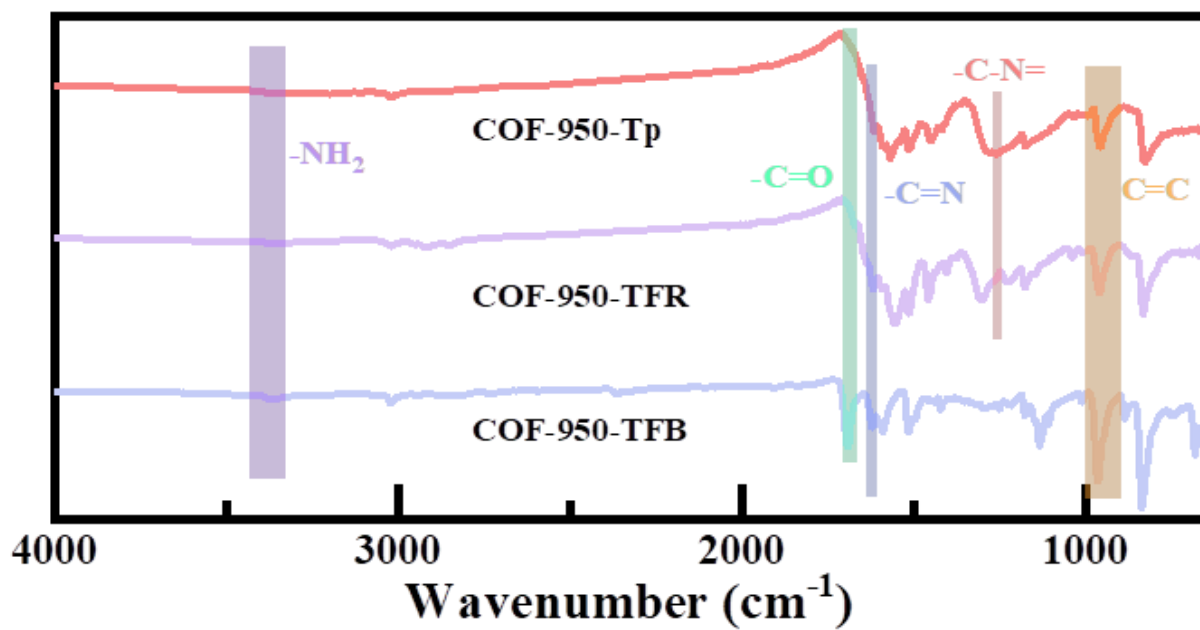


Figure S31. FTIR of COFs-950.

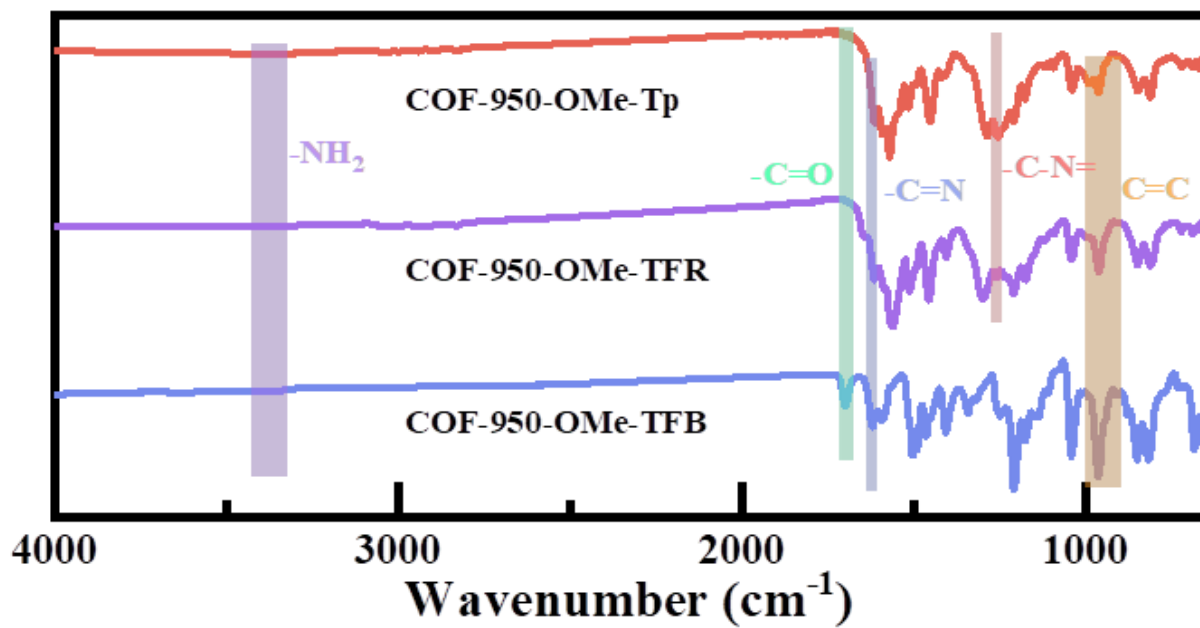


Figure S32. FTIR of COFs-950-OMe.

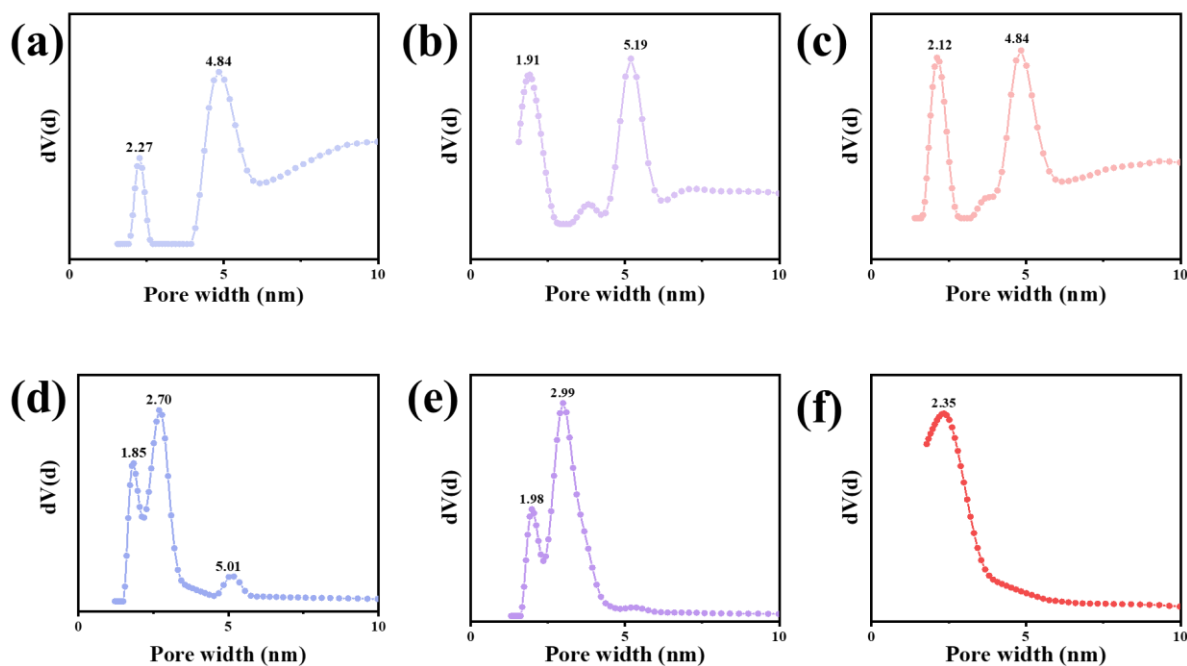


Figure S33. The pore distribution of all COFs: (a) COF-950-TFB, (b) COF-950-TFR, (c) COF-950-Tp, (d) COF-950-OMe-TFB, (e) COF-950-OMe-TFR, (f) COF-950-OMe-Tp.

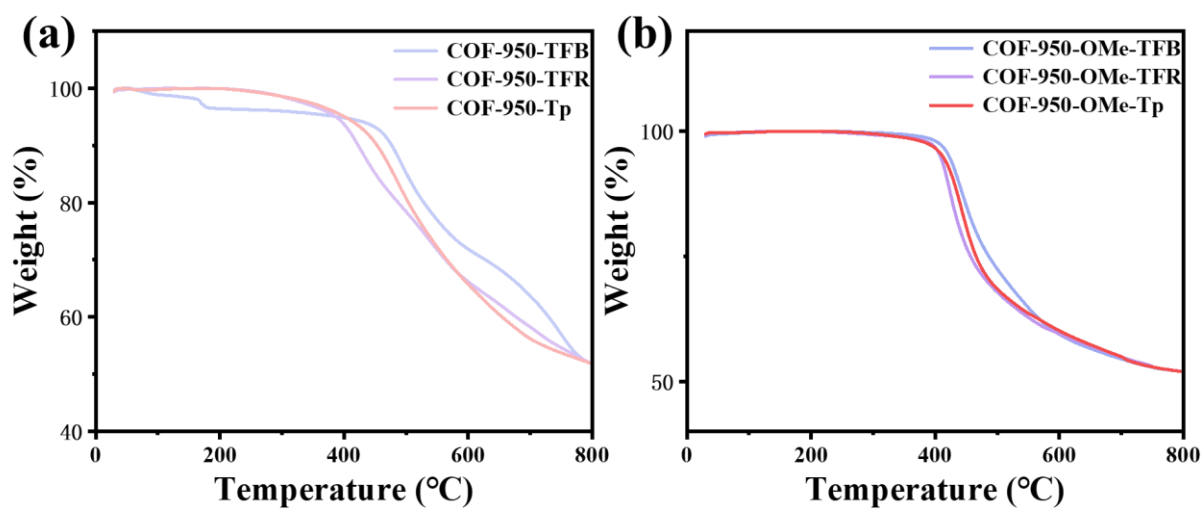


Figure S34. TGA profiles of (a) COFs-950, (b) COFs-950-OMe.

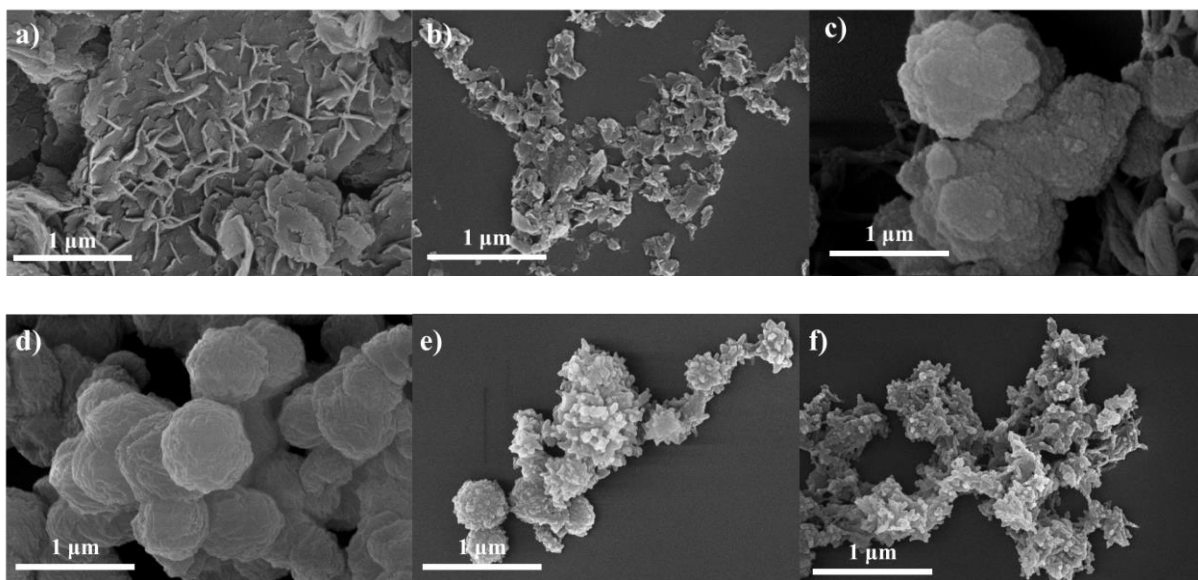


Figure S35. SEM images of all COFs: (a) COF-950-TFB, (b) COF-950-TFR, (c) COF-950-Tp, (d) COF-950-OMe-TFB, (e) COF-950-OMe-TFR, (f) COF-950-OMe-Tp.

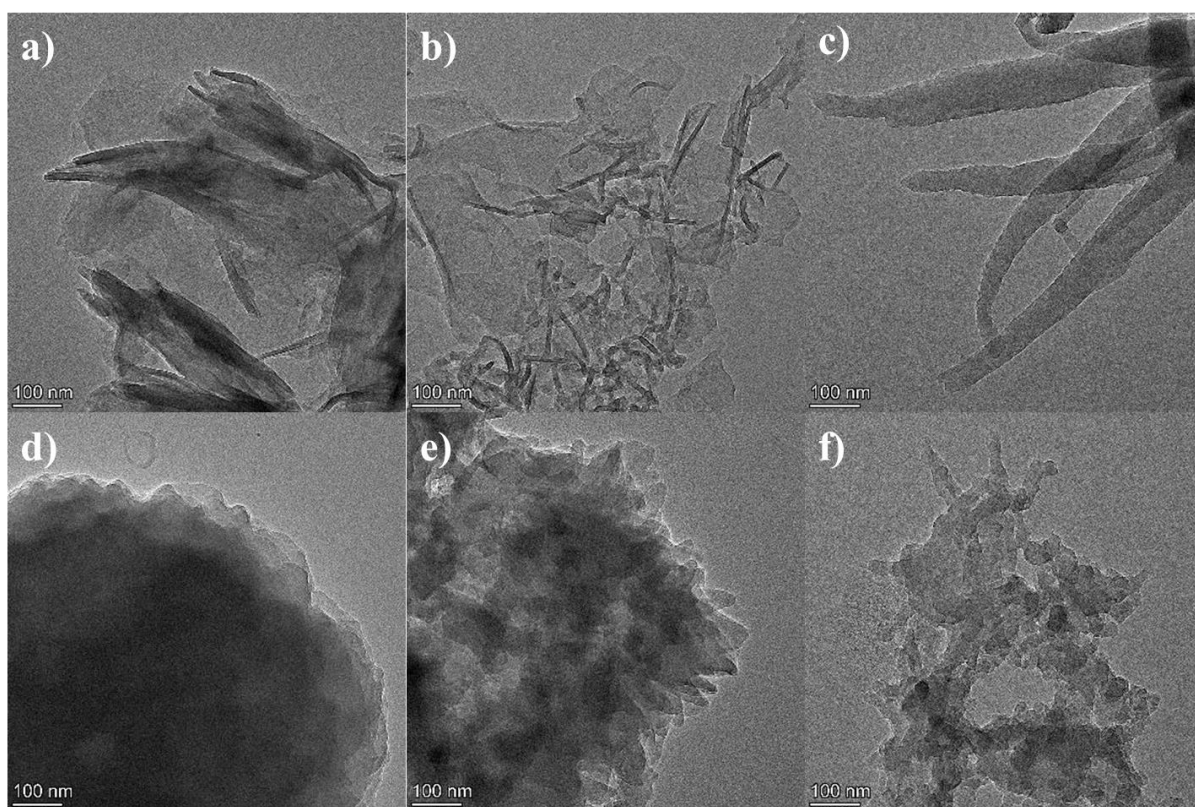


Figure S36. TEM images of all COFs: (a) COF-950-TFB, (b) COF-950-TFR, (c) COF-950-Tp, (d) COF-950-OMe-TFB, (e) COF-950-OMe-TFR, (f) COF-950-OMe-Tp.

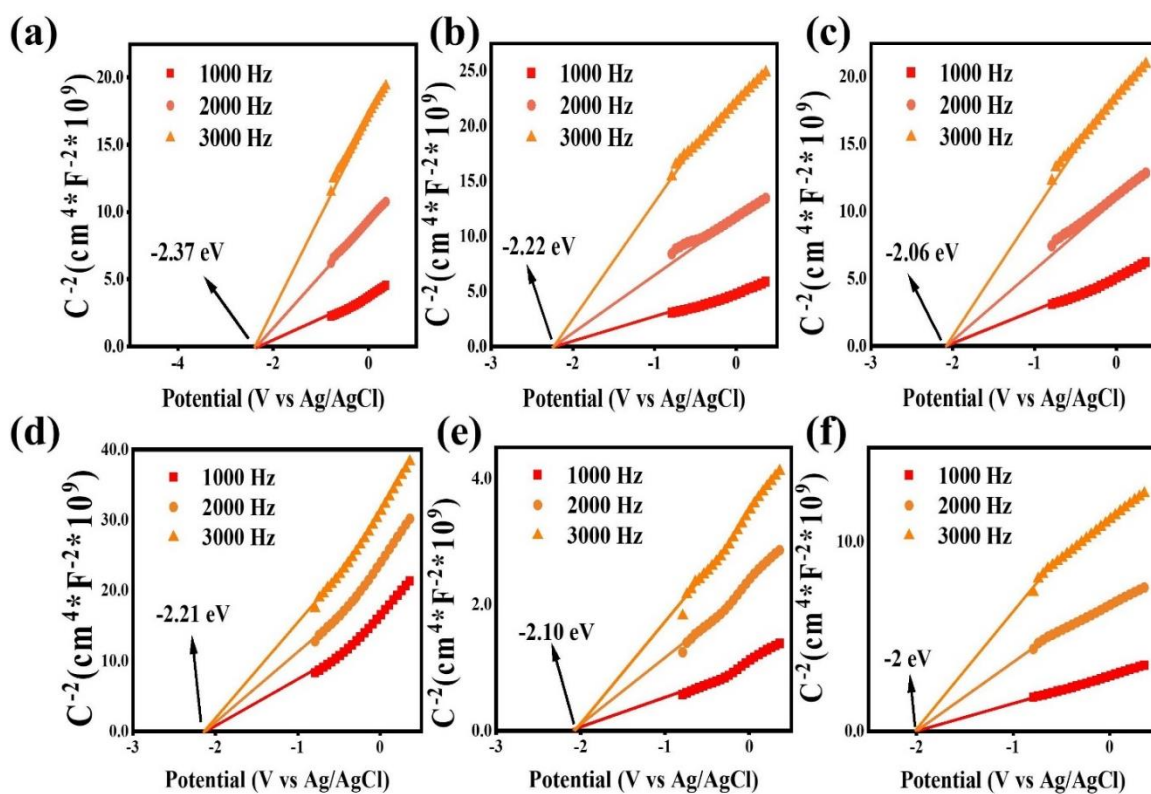


Figure S37. Mott–Schottky plots of all COFs: (a) COF-950-TFB, (b) COF-950-TFR, (c) COF-950-Tp, (d) COF-950-OMe-TFB, (e) COF-950-OMe-TFR, (f) COF-950-OMe-Tp.

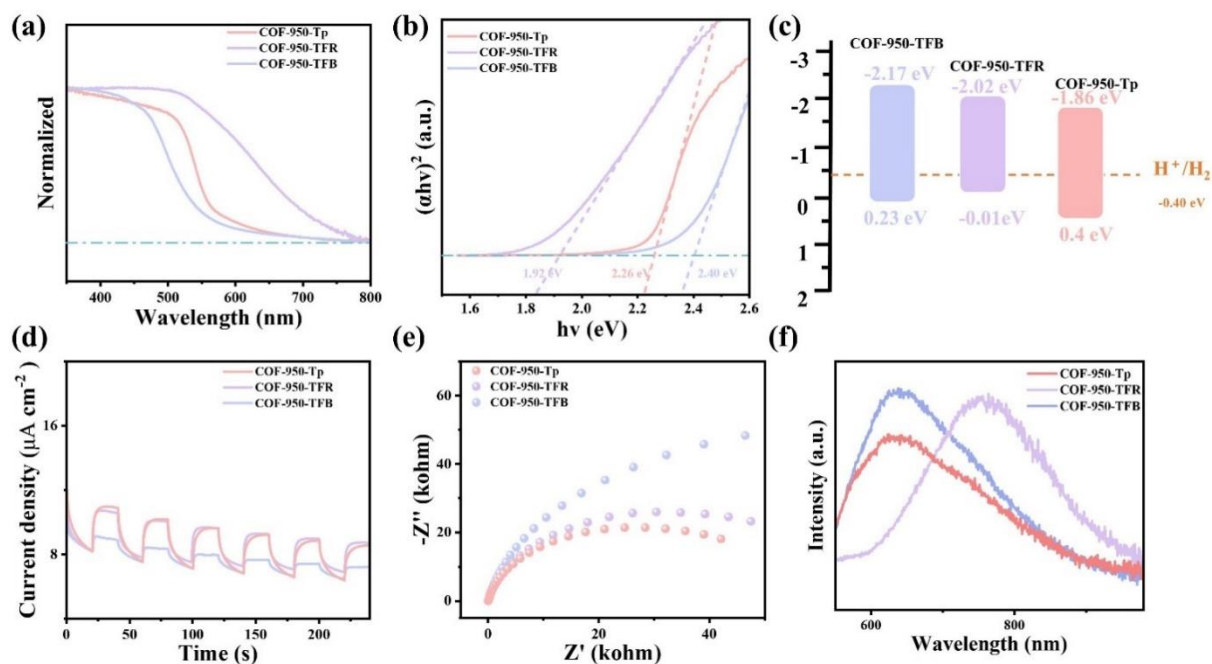


Figure S38. (a) UV-vis absorption spectra for COFs-950; (b) Tauc plots of COFs-950; (c) band structure of COFs-950; (d) Transient photocurrent responses of COFs-950 under irradiation with visible light; (e) Electrochemical impedance spectroscopy (EIS) Nyquist plots of COFs-950; (f) Steady-state photoluminescence (PL) spectra of COFs-950

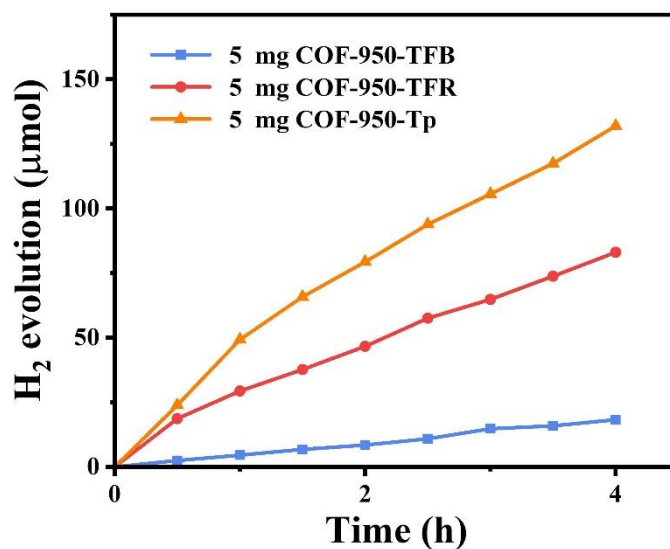


Figure S39. Hydrogen evolution rates for COFs-950.

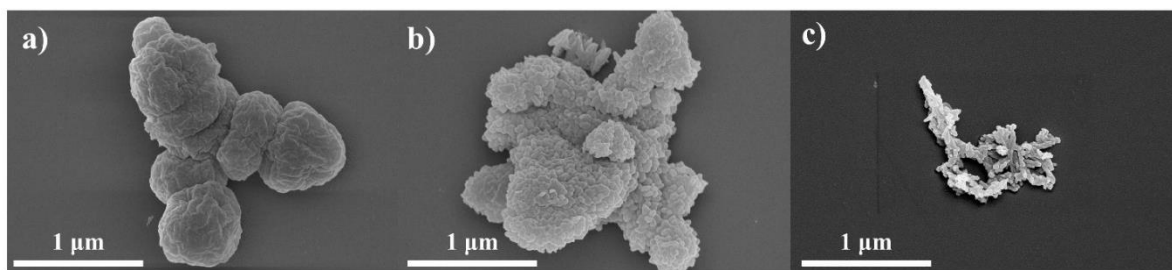


Figure S40. SEM images of recycle COFs-950-OMe: a) COF-950-OMe-TFB, b) COF-950-OMe-TFR, c) COF-950-OMe-Tp.

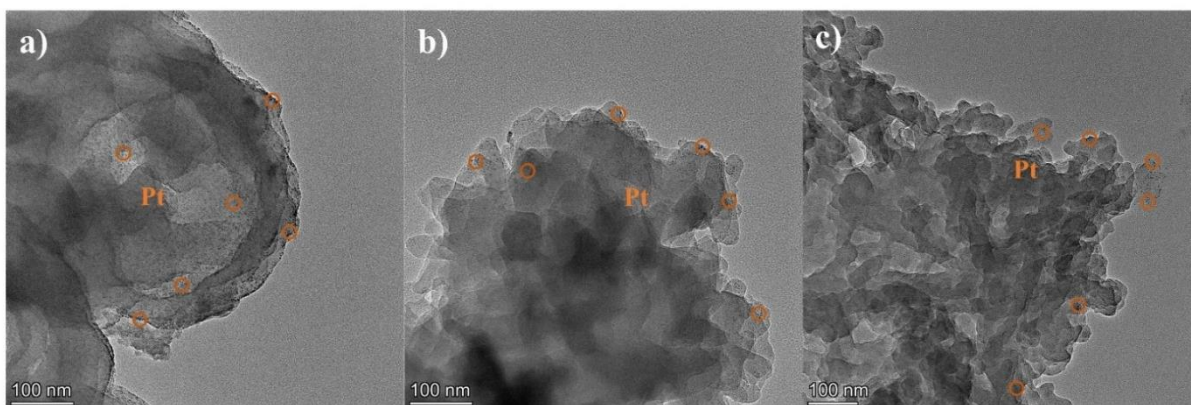


Figure S41 HR-TEM images of recycle COFs-950-OMe, Pt nanoparticles were observed: a) COF-950-OMe-TFB, b) COF-950-OMe-TFR, c) COF-950-OMe-Tp.

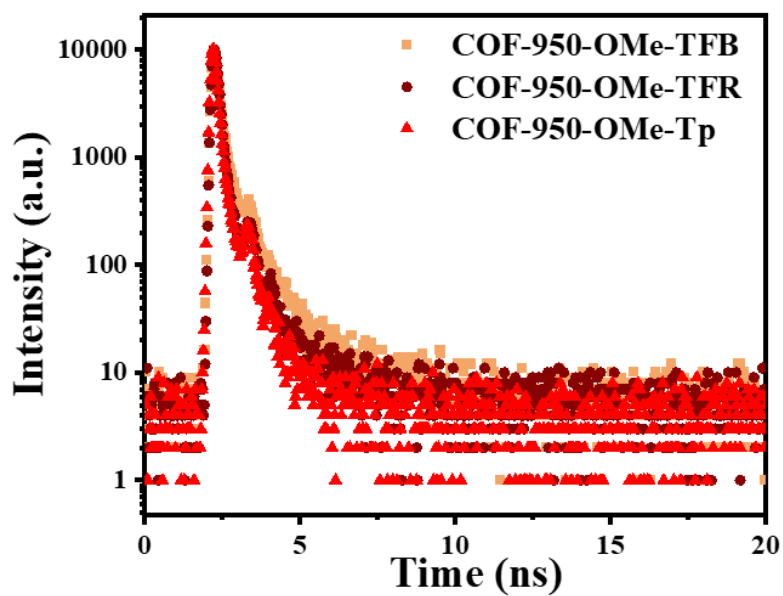


Figure S42 Time-resolved photoluminescence (TRPL) spectroscopy of COFs-950-OMe.

Section S4. Electrochemical measurements

Indium-tin oxide (ITO) glasses were firstly cleaned by sonication in ethanol and acetone for 30 min and dried under nitrogen flow. 5 mg of COF powder was mixed with 1 mL ethanol and ultra-sonicated for 30 min to get a slurry. Then 50 μ L 5% Nafion was added into the slurry for another 30 min ultra-sonication. The slurry was spreading onto ITO glass. After air drying, the boundary of the electrode was covered with an effective area of 1 cm². A conventional three electrodes cell was used with a platinum sheet (1 cm²) as the counter electrode and an Ag/AgCl electrode (saturated KCl) as reference electrode. The electrolyte was a 0.2 M Na₂SO₄ aqueous solution (pH 6.8). The working electrodes were immersed in the electrolyte for 60 s before any measurements were taken. The photocurrent measurements were conducted with a CHI760e workstation, with the working electrodes irradiated from the front side. The visible light was generated by a 300W xenon lamp (CEL-HXF300, Beijing China Education Au-light Co., Ltd) with a 420 nm cut-off filter, and was chopped manually. For Mott-Schottky experiments, the perturbation signal was 5 mV with the frequency from 1000-5000 Hz. The electrochemical impedance spectra (EIS) were performed in dark at open-circuit voltage with AC amplitude of 5 mV in the frequencies range of 0.1 Hz to 10⁵ Hz.

The applied potential vs. Ag/AgCl is converted to RHE potentials using the following equation:

$$E_{RHE} = E_{Ag/AgCl} + 0.0591 pH + E_{Ag/AgCl}^{\theta} \quad (E_{Ag/AgCl}^{\theta} = 0.199 V)$$

Tauc plot.

It is used to determine the optical bandgap of a semiconductor material. The plot is constructed by plotting the absorption coefficient (α) against the photon energy ($h\nu$). And it is a linear plot that can be extrapolated to the x-axis to determine the energy bandgap (E_g) of the material.

$$(ah\nu)^{1/n} = A(h\nu - E_g)$$

Section S5. Photocatalytic measurements

Photocatalytic hydrogen evolution reaction measurements

5 mg photocatalyst was dispersed into 50 mL 0.1 M ascorbic acid solution and then added into the

photoreactor. Then the resulting suspension was ultrasonicated for 30 min to obtain a well dispersed suspension. Pt was loaded on the surface of the photocatalyst by using H_2PtCl_6 in the in situ photodeposition approach. We evacuated the mixture several times to remove air completely before irradiation under a 300 W Xe-lamp and a water-cooling filter. The temperature of the reaction solution was kept at room temperature by a flow of cooling water. The generated gases were analyzed by gas chromatography equipped with a thermal conductive detector (TCD) with argon as the carrier gas. The light resource was changed by using different cut-off filters. A 420 nm cut-off filter was used to obtain visible light.

AQY measurements

Apparent quantum efficiency (AQY) measurements were performed under monochromatic irradiation, generated from a 300 W Xe lamp equipped with bandpass filters (central wavelength: 420, 450, 520, 550, 600 700 nm; full width at half maximum: 10 nm). Monochromatic photon fluxes at each wavelength were measured using an optical photodiode power meter (CEL-NP2000), the intensities were 75, 78, 73, 72, 81 W m^{-2} , respectively. The AQY was calculated using the following equation:

$$AQY = \frac{N_e}{N_p} \times 100\% = \frac{10^9(v \times N_A \times n) \times (h \times c)}{P \times A \times \lambda} \times 100\%$$

Where, N_e is the amount of generated electron, N_p is the incident photons, v is the H_2 evolution rate (mol s^{-1}), N_A is Avogadro constant ($6.022 \times 10^{23} \text{ mol}^{-1}$), n is number of transferred electrons in hydrogen evolution reaction (2), h is the Planck constant ($6.626 \times 10^{-34} \text{ J s}$), c is the speed of light ($3 \times 10^8 \text{ m s}^{-1}$), P is the intensity of irradiation light (W m^{-2}), A is the irradiation area (m^2), t is the photoreaction time (s), λ is the wavelength of the monochromatic light (nm).

Section S6. Density functional theory (DFT) calculations

Quantum chemical studies were performed using density functional theory (DFT) implemented in GAUSSIAN 09 package. Geometry optimization and frequency analysis were calculated at B3LYP hybrid functional under the level of 6-31G* basis sets.

Section S7. Structural simulation

Molecular modeling of all COFs was generated with the Materials Studio (ver. 8.0) suite of programs. Pawley refinement was carried out using Reflex, a software package for crystal determination from PXRD pattern. Unit cell dimension was set to the theoretical parameters. The Pawley refinement was performed to optimize the lattice parameters iteratively until the R_{wp} value converges and the overlay observed with refined profiles shows good agreement. The lattice models (cell parameters, atomic positions, and total energy) were then fully optimized using Materials Studio Forcite molecular dynamics module method. P1 space group was chosen for the primitive models in the initial simulations.

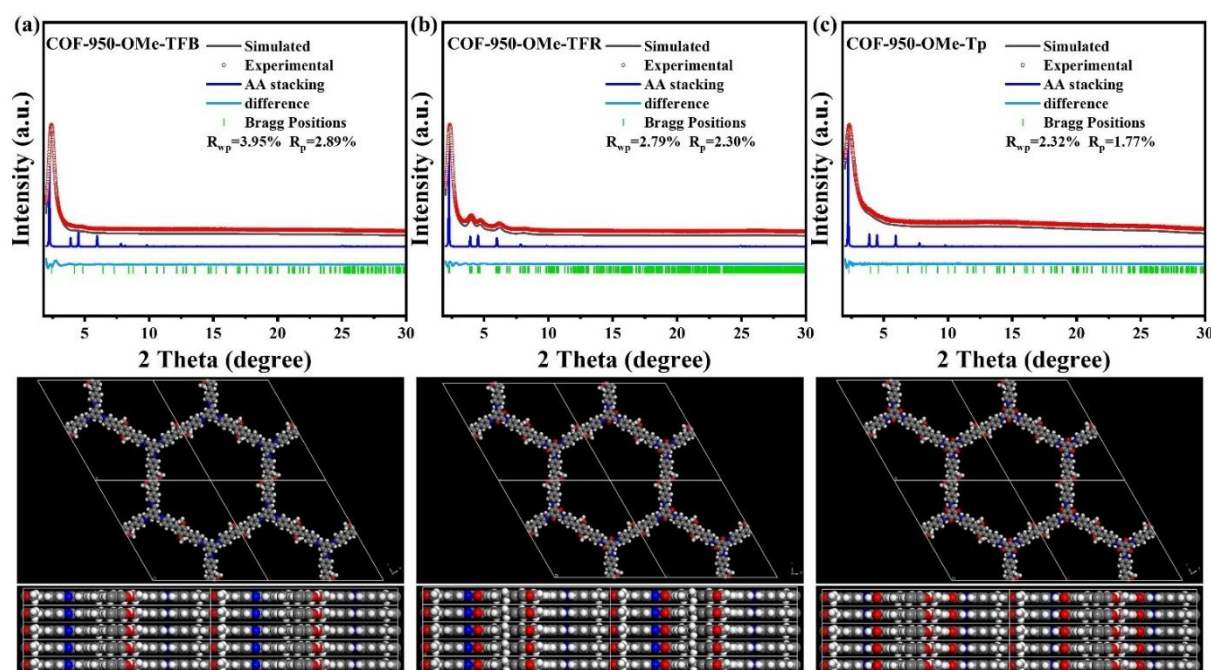


Figure S43. experimental and simulated PXRD patterns of COFs-950-OMe.

Table S1. The photocatalytic hydrogen evolution performance comparison of COFs in this study with other OPV-based COFs under visible light sunlight.

COF	Co-catalyst	Sacrificial agent	Range of visible light irradiation (nm)	Activity (mmol·g ⁻¹ ·h ⁻¹)	ref.
COF-950-OMe-Tp	Pt (3 wt%)	ascorbic acid	420-780	24.19	This work
COF-950-OMe-TFR	Pt (3 wt%)	ascorbic acid	420-780	10.42	This work
COF-950-OMe-TFB	Pt (3 wt%)	ascorbic acid	420-780	2.89	This work
COF-960-0	Pt (3 wt%)	ascorbic acid	420-780	0.219	J. Mater. Chem. A, 2023, 11, 14760–14767
COF-960-1	Pt (3 wt%)	ascorbic acid	420-780	0.318	J. Mater. Chem. A, 2023, 11, 14760–14767
COF-960-2	Pt (3 wt%)	ascorbic acid	420-780	0.338	J. Mater. Chem. A, 2023, 11, 14760–14767
COF-960-3	Pt (3 wt%)	ascorbic acid	420-780	0.386	J. Mater. Chem. A, 2023, 11, 14760–14767
COF-960-4	Pt (3 wt%)	ascorbic acid	420-780	0.643	J. Mater. Chem. A, 2023, 11, 14760–14767
COF-960-5	Pt (3 wt%)	ascorbic acid	420-780	0.678	J. Mater. Chem. A, 2023, 11, 14760–14767
COF-960-6	Pt (3 wt%)	ascorbic acid	420-780	0.539	J. Mater. Chem. A, 2023, 11, 14760–14767
COF-932	Pt (3 wt%)	ascorbic acid	350-780	0.73	Angew. Chem. Int. Ed. 2023, 62, e202216073
COF-923	Pt (3 wt%)	ascorbic acid	350-780	23.4	Angew. Chem. Int. Ed. 2023, 62, e202216073
COF-935	Pt (3 wt%)	ascorbic acid	420-780	67.55	Angew. Chem. Int. Ed. 2023, 62, e202304611
COF-953	Pt (5 wt%)	ascorbic acid	420-780	60.53	Adv. Mater. 2024, 36, 2308251
COF-954	Pt (5 wt%)	ascorbic acid	420-780	137.23	Adv. Mater. 2024, 36, 2308251

Table S2. Unit cell parameters and fractional atomic coordinates for COF-950-OMe-TFB based on the AA-stacking.

Space group	P6 (No. 168)		
Calculated unit cell	a = b = 45.2313 Å, c = 3.5681 Å		
	$\alpha = \beta = 90^\circ, \gamma = 120^\circ$		
Atom	x/a	y/b	z/c
C1	4.67872	-0.6897	0.5
C2	4.6435	-0.70187	0.5
C3	4.61877	-0.73853	0.5
N4	4.62857	-0.76099	0.5
C5	4.60523	-0.79699	0.5
C6	4.56973	-0.81038	0.5
C7	4.54763	-0.84563	0.5
C8	4.56068	-0.86785	0.5
C9	4.59613	-0.8545	0.5
C10	4.61823	-0.81926	0.5
C11	4.53674	-0.90469	0.5
C12	4.54711	-0.92751	0.5
C13	4.52347	-0.96458	0.5
C14	4.53549	-0.98811	0.5
O15	4.57014	-0.9788	0.5
C16	4.59256	-0.94989	0.5
C17	4.48819	-0.977	0.5
H18	4.68862	-0.70845	0.5
H19	4.59024	-0.74781	0.5
H20	4.55886	-0.79243	0.5
H21	4.51884	-0.85637	0.5
H22	4.60698	-0.87247	0.5
H23	4.64703	-0.80852	0.5
H24	4.50806	-0.91474	0.5
H25	4.57556	-0.91863	0.5
H26	4.59765	-0.93971	0.20068
H27	4.61668	-0.94827	0.6203
H28	4.58486	-0.93396	0.67902
H29	4.47809	-0.95842	0.5

Table S3. Unit cell parameters and fractional atomic coordinates for COF-950-OMe-TFR based on the AA-stacking.

Space group	P1(1)		
Calculated unit cell	a = 43.7554 Å, b = 45.5579 Å, c = 3.55944 Å		
	$\alpha = \gamma = 90^\circ, \beta = 120^\circ$		
Atom	x/a	y/b	z/c
C1	0.68103	0.31042	0.5
C2	0.64354	0.29585	0.5
C3	0.62162	0.26227	0.5
N4	0.63196	0.2373	0.5
C5	0.60835	0.2017	0.5
C6	0.57321	0.18921	0.5
C7	0.55064	0.1543	0.5
C8	0.5629	0.13157	0.5
C9	0.59805	0.14408	0.5
C10	0.62063	0.17899	0.5
C11	0.53848	0.09509	0.5
C12	0.54811	0.07184	0.5
C13	0.52395	0.03511	0.5
C14	0.48897	0.02348	0.5
C15	0.53518	0.01109	0.5
O16	0.56947	0.0196	0.5
C17	0.59228	0.04835	0.5
C18	0.68958	0.37061	0.5
C19	0.70415	0.34769	0.5
C20	0.73773	0.35935	0.5
N21	0.7627	0.39466	0.5
C22	0.7983	0.40665	0.5
C23	0.81079	0.38401	0.5
C24	0.8457	0.39634	0.5
C25	0.86843	0.43133	0.5
C26	0.85592	0.45397	0.5
C27	0.82101	0.44164	0.5
C28	0.90491	0.44338	0.5
C29	0.92816	0.47626	0.5
C30	0.96489	0.48884	0.5
C31	0.97652	0.46549	0.5
C32	0.98891	0.52409	0.5
O33	0.70829	0.4014	0.5
O34	0.9804	0.54987	0.5
C35	0.95165	0.54393	0.5
C36	0.62939	0.31897	0.5
C37	0.65231	0.35646	0.5
C38	0.64065	0.37838	0.5
N39	0.60534	0.36804	0.5
C40	0.59335	0.39165	0.5
C41	0.61599	0.42679	0.5
C42	0.60366	0.44936	0.5

C43	0.56867	0.4371	0.5
C44	0.54603	0.40195	0.5
C45	0.55836	0.37937	0.5
C46	0.55662	0.46152	0.5
C47	0.52374	0.45189	0.5
C48	0.51116	0.47605	0.5
C49	0.53451	0.51103	0.5
C50	0.47591	0.46482	0.5
O51	0.5986	0.30689	0.5
O52	0.45013	0.43053	0.5
C53	0.45607	0.40772	0.5
C54	0.31897	0.68958	0.5
C55	0.35646	0.70415	0.5
C56	0.37838	0.73773	0.5
N57	0.36804	0.7627	0.5
C58	0.39165	0.7983	0.5
C59	0.42679	0.81079	0.5
C60	0.44936	0.8457	0.5
C61	0.4371	0.86843	0.5
C62	0.40195	0.85592	0.5
C63	0.37937	0.82101	0.5
C64	0.46152	0.90491	0.5
C65	0.45189	0.92816	0.5
C66	0.47605	0.96489	0.5
C67	0.51103	0.97652	0.5
C68	0.46482	0.98891	0.5
O69	0.43053	0.9804	0.5
C70	0.40772	0.95165	0.5
C71	0.31042	0.62939	0.5
C72	0.29585	0.65231	0.5
C73	0.26227	0.64065	0.5
N74	0.2373	0.60534	0.5
C75	0.2017	0.59335	0.5
C76	0.18921	0.61599	0.5
C77	0.1543	0.60366	0.5
C78	0.13157	0.56867	0.5
C79	0.14408	0.54603	0.5
C80	0.17899	0.55836	0.5
C81	0.09509	0.55662	0.5
C82	0.07184	0.52374	0.5
C83	0.03511	0.51116	0.5
C84	0.02348	0.53451	0.5
C85	0.01109	0.47591	0.5
O86	0.29171	0.5986	0.5
O87	0.0196	0.45013	0.5
C88	0.04835	0.45607	0.5
C89	0.37061	0.68103	0.5
C90	0.34769	0.64354	0.5
C91	0.35935	0.62162	0.5
N92	0.39466	0.63196	0.5
C93	0.40665	0.60835	0.5

C94	0.38401	0.57321	0.5
C95	0.39634	0.55064	0.5
C96	0.43133	0.5629	0.5
C97	0.45397	0.59805	0.5
C98	0.44164	0.62063	0.5
C99	0.44338	0.53848	0.5
C100	0.47626	0.54811	0.5
C101	0.48884	0.52395	0.5
C102	0.46549	0.48897	0.5
C103	0.52409	0.53518	0.5
O104	0.4014	0.69311	0.5
O105	0.54987	0.56947	0.5
C106	0.54393	0.59228	0.5
H107	0.6922	0.29286	0.5
H108	0.59308	0.25235	0.5
H109	0.65939	0.24533	0.5
H110	0.56305	0.20763	0.5
H111	0.52207	0.1442	0.5
H112	0.60822	0.12567	0.5
H113	0.64919	0.18909	0.5
H114	0.51004	0.0857	0.5
H115	0.57629	0.08009	0.5
H116	0.47951	0.04246	0.5
H117	0.59736	0.05855	0.19994
H118	0.61612	0.04943	0.61848
H119	0.58512	0.0645	0.68157
H120	0.74765	0.34073	0.5
H121	0.79237	0.35543	0.5
H122	0.8558	0.37787	0.5
H123	0.87433	0.48256	0.5
H124	0.81091	0.46011	0.5
H125	0.9143	0.42435	0.5
H126	0.91991	0.49619	0.5
H127	0.95754	0.43704	0.5
H128	0.9341	0.51636	0.58612
H129	0.94454	0.54827	0.20603
H130	0.94887	0.56149	0.70785
H131	0.65927	0.40692	0.5
H132	0.58594	0.34061	0.5
H133	0.64457	0.43695	0.5
H134	0.62213	0.47793	0.5
H135	0.51744	0.39178	0.5
H136	0.53989	0.35081	0.5
H137	0.57565	0.48996	0.5
H138	0.50381	0.42371	0.5
H139	0.56296	0.52049	0.5
H140	0.44927	0.39462	0.21408
H141	0.44036	0.38862	0.72786
H142	0.48425	0.41815	0.55806
H143	0.3078	0.70714	0.5
H144	0.40692	0.74765	0.5

H145	0.34061	0.75467	0.5
H146	0.43695	0.79237	0.5
H147	0.47793	0.8558	0.5
H148	0.39178	0.87433	0.5
H149	0.35081	0.81091	0.5
H150	0.48996	0.9143	0.5
H151	0.42371	0.91991	0.5
H152	0.52049	0.95754	0.5
H153	0.41705	0.93444	0.61848
H154	0.39829	0.94356	0.19994
H155	0.38605	0.94951	0.68157
H156	0.25235	0.65927	0.5
H157	0.20763	0.64457	0.5
H158	0.1442	0.62213	0.5
H159	0.12567	0.51744	0.5
H160	0.18909	0.53989	0.5
H161	0.0857	0.57565	0.5
H162	0.08009	0.50381	0.5
H163	0.04246	0.56296	0.5
H164	0.05953	0.46419	0.20603
H165	0.04909	0.43228	0.58612
H166	0.06386	0.47741	0.70785
H167	0.34073	0.59308	0.5
H168	0.41406	0.65939	0.5
H169	0.35543	0.56305	0.5
H170	0.37787	0.52207	0.5
H171	0.48256	0.60822	0.5
H172	0.46011	0.64919	0.5
H173	0.42435	0.51004	0.5
H174	0.49619	0.57629	0.5
H175	0.43704	0.47951	0.5
H176	0.52444	0.58769	0.72786
H177	0.53335	0.59369	0.21408
H178	0.56833	0.61723	0.55806

Table S4. Unit cell parameters and fractional atomic coordinates for COF-950-OMe-Tp based on the AA-stacking.

Space group	P6/M (No. 175)		
Calculated unit cell	a = b = 49.6385 Å, c = 4.8722 Å		
	$\alpha = \beta = 90^\circ, \gamma = 120^\circ$		
Atom	x/a	y/b	z/c
C1	1.68103	-2.68958	0.5
C2	1.64354	-2.70415	0.5
C3	1.62162	-2.73773	0.5
N4	1.63196	-2.7627	0.5
C5	1.60835	-2.7983	0.5
C6	1.57321	-2.81079	0.5
C7	1.55064	-2.8457	0.5
C8	1.5629	-2.86843	0.5
C9	1.59805	-2.85592	0.5
C10	1.62063	-2.82101	0.5
C11	1.53848	-2.90491	0.5
C12	1.54811	-2.92816	0.5
C13	1.52395	-2.96489	0.5
C14	1.48897	-2.97652	0.5
C15	1.53518	-2.98891	0.5
O16	1.69311	-2.70829	0.5
O17	1.56947	-2.9804	0.5
C18	1.59228	-2.95165	0.5
H19	1.59308	-2.74765	0.5
H20	1.65939	-2.75467	0.5
H21	1.56305	-2.79237	0.5
H22	1.52207	-2.8558	0.5
H23	1.60822	-2.87433	0.5
H24	1.64919	-2.81091	0.5
H25	1.51004	-2.9143	0.5
H26	1.57629	-2.91991	0.5
H27	1.47951	-2.95754	0.5
H28	1.59736	-2.94145	0.19994
H29	1.61612	-2.95057	0.61848
H30	1.58512	-2.9355	0.68157

Reference

- 1 Y. Zhong, W. Dong, S. Ren and L. Li, *Adv. Mater.*, 2024, **36**, 2308251.
- 2 S. E. Estrada, C. Ochoa-Puentes and C. A. Sierra, *J. Mol. Struct.*, 2017, **1133**, 448–457.
- 3 N. Kaur, J.-G. Delcros, J. Imran, A. Khaled, M. Chehtane, N. Tschammer, B. Martin and O. I. Phanstiel, *J. Med. Chem.*, 2008, **51**, 1393–1401.
- 4 S. H. M. Mehr, H. Depmeier, K. Fukuyama, M. Maghami and M. J. MacLachlan, *Org. Biomol. Chem.*, 2017, **15**, 581–583.
- 5 J. H. Chong, M. Sauer, B. O. Patrick and M. J. MacLachlan, *Org. Lett.*, 2003, **5**, 3823–3826.